confirmed that these cytokines show their maximum fibroproliferative effects at these concentrations (data not shown) and our results were consistent with previous studies [18–20]. In addition, the proliferative activities of CCD-11Lu in the presence of certain concentrations of these cytokines accompanied by 100 U/ml of KL-6 were also assessed. Results were expressed as values relative to those obtained from the cells cultured in the absence of any cytokines or KL-6.

Statistical analysis. All experiments were performed in triplicate. Data are expressed as means ± SD. Differences between two categories were analyzed using Student's t test and the Mann–Whitney's U test. Data obtained from the experiments using various concentrations of the reagents (KL-6 and anti-KL-6 mAb) were evaluated using one-way analysis of variance (ANOVA). A p value <0.05 was considered statistically significant.

Results

KL-6 accelerates proliferation of human lung fibroblasts

The presence of 100 U/ml of KL-6 in the culture medium was found to accelerate cell proliferation in all of seven human lung fibroblasts examined (Table 1). CCD-11Lu fibroblasts were selected for further experiments based on the strength of their response to KL-6. As shown in Fig. 1A, the presence of KL-6 from 1 to 1000 U/ml accelerated the proliferation of CCD-11Lu in a dose-dependent manner. Furthermore, addition of anti-KL-6 mAb inhibited the KL-6-induced proliferation of CCD-11Lu in a dose-dependent manner, and 100 μg/ml of anti-KL-6 mAb completely counteracted the proliferation of CCD-11Lu induced by 100 U/ml of KL-6 (Fig. 1B). To further confirm the effect of KL-6 on the proliferative activity of human fibroblasts, we examined DNA synthesis in the presence of 100 U/ml of KL-6. As shown in Fig. 1C, BrdU incorporation was augmented in CCD-11Lu that were cultured in medium containing KL-6 and this enhancement was attenuated by the addition of anti-KL-6 mAb.

Table 1
Effects of KL-6 on the proliferation of fibroblasts

Cell line	MTS absorbance[a]		Promotion index[b]
	control	KL-6 (100 U/ml)	
CCD-11Lu[c]	0.43 ± 0.02	0.54 ± 0.01*	1.26
CCD-13Lu[c]	0.47 ± 0.00	0.53 ± 0.00*	1.13
CCD-16Lu[c]	0.40 ± 0.01	0.48 ± 0.02*	1.20
CCD-18Lu[c]	0.44 ± 0.01	0.53 ± 0.04*	1.21
WI-38[c]	0.56 ± 0.02	0.68 ± 0.01*	1.22
MRC-5[c]	0.46 ± 0.00	0.55 ± 0.04*	1.20
MRC-9[c]	0.34 ± 0.01	0.42 ± 0.02*	1.24
3T3[d]	0.43 ± 0.00	0.41 ± 0.03	0.97
A-9[e]	0.31 ± 0.01	0.30 ± 0.01	0.98

[a] MTS absorbance was measured in the absence of KL-6, which was designated as a control. Data were determined in triplicate and are represented as means ± SD.
[b] Promotion index = relative value of MTS absorbance evaluated in the presence of KL-6 in comparison to control.
[c] Human lung fibroblast.
[d] Mouse lung fibroblast.
[e] Mouse skin fibroblast.
* $P < 0.05$ vs control, Student's t test.

KL-6 has an anti-apoptotic effect on human lung fibroblasts

Significantly more CCD-11Lu survived apoptosis in the presence of KL-6 at concentrations ranging from 10 to 1000 U/ml, and the survival was a function of the KL-6 concentration (Fig. 2A). The anti-apoptotic effect of KL-6 on CCD-11Lu was shown to be attenuated by anti-KL-6 mAb in a dose-dependent manner, and 100 μg/ml of anti-KL-6 mAb completely attenuated the anti-apoptotic effect of 100 U/ml of KL-6 on CCD-11Lu (Fig. 2B). Other human lung fibroblasts (CCD-16Lu and WI-38) were also examined, and similar results were obtained (data not shown). To confirm the anti-apoptotic effect of KL-6 on human lung fibroblasts, we quantified viable cells in CCD-11Lu in the presence or absence of 100 U/ml of KL-6 at 4, 6, 8, 10, and 12 h after inducing apoptosis with an anti-Fas mAb and cycloheximide. As shown in Fig. 2C, significantly more viable cells were found as early as 8 h after inducing apoptosis in the group to which KL-6 was added than in the group without KL-6, and this trend persisted until observation was stopped 12 h after apoptotic induction.

Anti-apoptotic effect of KL-6 on human lung fibroblasts is confirmed by morphological and immunohistological assessments

Apoptotic fibroblasts characterized by chromatin concentration, cytomembrane shrinkage, or neighboring cell detachment were examined by Diff-Quik staining and Hoechst 33324 staining. DNA fragmentation, which is another indicator of apoptosis was assessed by TUNEL staining. As shown in Fig. 3, the presence of KL-6 in the culture medium was found to decrease apoptotic fibroblasts. Furthermore, the number of TUNEL-positive fibroblasts was significantly lower in the group treated with KL-6 compared to the group without KL-6 (Fig. 4).

KL-6 augments proliferative effect of bFGF, PDGF-BB, and TGF-β on human lung fibroblasts

Every cytokine induced proliferation of CCD-11Lu, which was consistent with previous studies [21–24]. Among the cytokines examined, bFGF showed the strongest proliferation-promoting effect: 48 h of co-incubation with 100 ng/ml of bFGF resulted in a 43.9% promotion of proliferation, while incubation with KL-6 (100 and 1000 U/ml) was 26.0% and 31.9%, respectively (Fig. 5A). In addition, 100 U/ml of purified KL-6 showed an additive effect on proliferation promoted by each cytokine examined (Fig. 5C).

KL-6 has a stronger anti-apoptotic effect compared to that of bFGF, PDGF-BB, and TGF-β on human lung fibroblasts

KL-6 showed a stronger ability to protect CCD-11Lu from apoptosis than bFGF, PDGF-BB, and TGF-β: 100

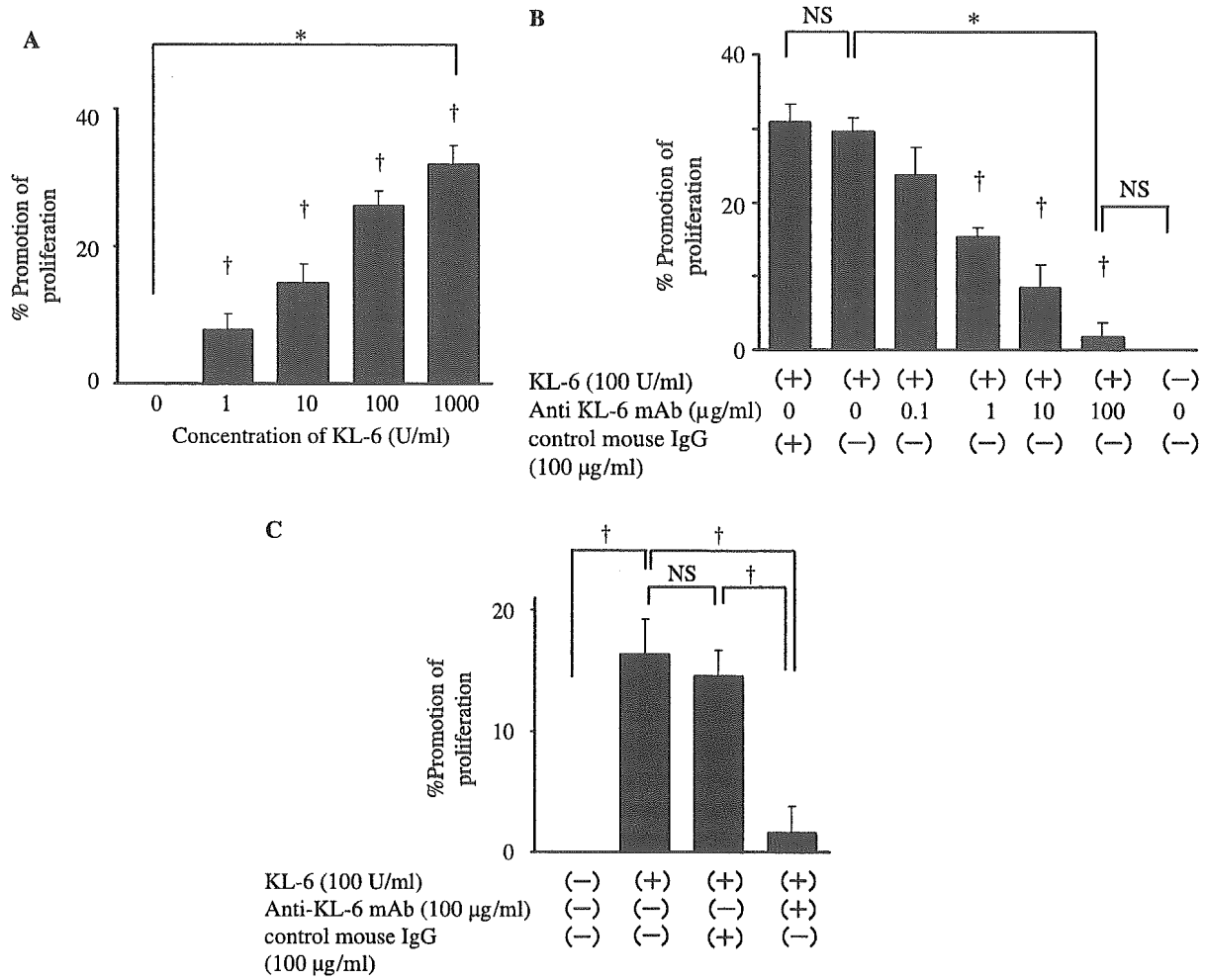

Fig. 1. Effect of KL-6 and anti-KL-6 mAb on the proliferation of CCD-11Lu fibroblasts. Proliferative activity was expressed as a promotion index, a relative value of MTS absorbance measured from the cells cultured in the presence of KL-6 to that in the absence of KL-6. MTS absorbance, which indicates cell viability, was measured as described under Materials and methods. (A) Proliferative activity of CCD-11Lu was significantly augmented with increasing concentrations of KL-6 ($^*P < 0.0001$, one-way ANOVA). At KL-6 concentrations of 1, 10, 100, and 1000 U/ml proliferative activity was significantly higher than without KL-6 ($^\dagger P < 0.05$, Student's t test). (B) Accelerated proliferation of CCD-11Lu fibroblasts in the presence of 100 U/ml of KL-6 was blunted by the addition of anti-KL-6 mAb in a dose-dependent manner ($^*P < 0.0001$, one-way ANOVA). The inhibitory effect of anti-KL-6 mAb was statistically significant at concentration ranges from 1 to 100 μg/ml ($^\dagger P < 0.05$, Student's t test). Control mouse IgG had no effect. (C) Incorporation of BrdU into CCD-11Lu cultured in the presence of 100 U/ml of KL-6 was significantly higher than in the absence of KL-6, and this enhancement was attenuated by the addition of 100 μg/ml of anti-KL-6 mAb ($^\dagger P < 0.05$, Student's t test). Control mouse IgG had no effect. Data were determined in triplicate and expressed as means ± SD (A–C).

and 1000 U/ml of KL-6 resulted in a 15.0% and 19.4% inhibition of apoptosis, respectively (Fig. 5B). In addition, 100 U/ml of purified KL-6 showed an additive protective effect from the apoptosis induced by each cytokine examined (Fig. 5D).

Discussion

In the present study, we have demonstrated that KL-6 molecules have a pro-proliferative effect on all human lung fibroblasts that were examined in vitro. We also demonstrated that KL-6 has an anti-apoptotic effect in that it rescues lung fibroblasts from apoptosis induced by anti-Fas mAb and cycloheximide. In addition, we confirmed that addition of anti-KL-6 mAb to the cell culture blunted both the pro-proliferative and anti-apoptotic effects of KL-6 on CCD-11Lu cells in a dose-dependent manner, indicating that both effects are specific for the epitope of KL-6. The proliferative activity of KL-6 was comparable and additive to those of bFGF, PDGF, and TGF-β at concentrations reported to show the maximum effects in vitro. Furthermore, the anti-apoptotic effect of KL-6 was stronger than those of these cytokines and this effect was also additive. In ILD, the concentration of KL-6 in the ELF is reported to exceed 15,000 U/ml [5,8]. In the present study, however, the effects of KL-6 on the proliferation and survival of human lung fibroblasts were examined at the maximum concentration of 1000 U/ml, because of technical problems in purification of KL-6. Taken together with our previous study demonstrating the chemotactic activity of KL-6 on fibroblasts [16], these results indicate that large amounts of the KL-6 molecule in the alveolar spaces of IPF might

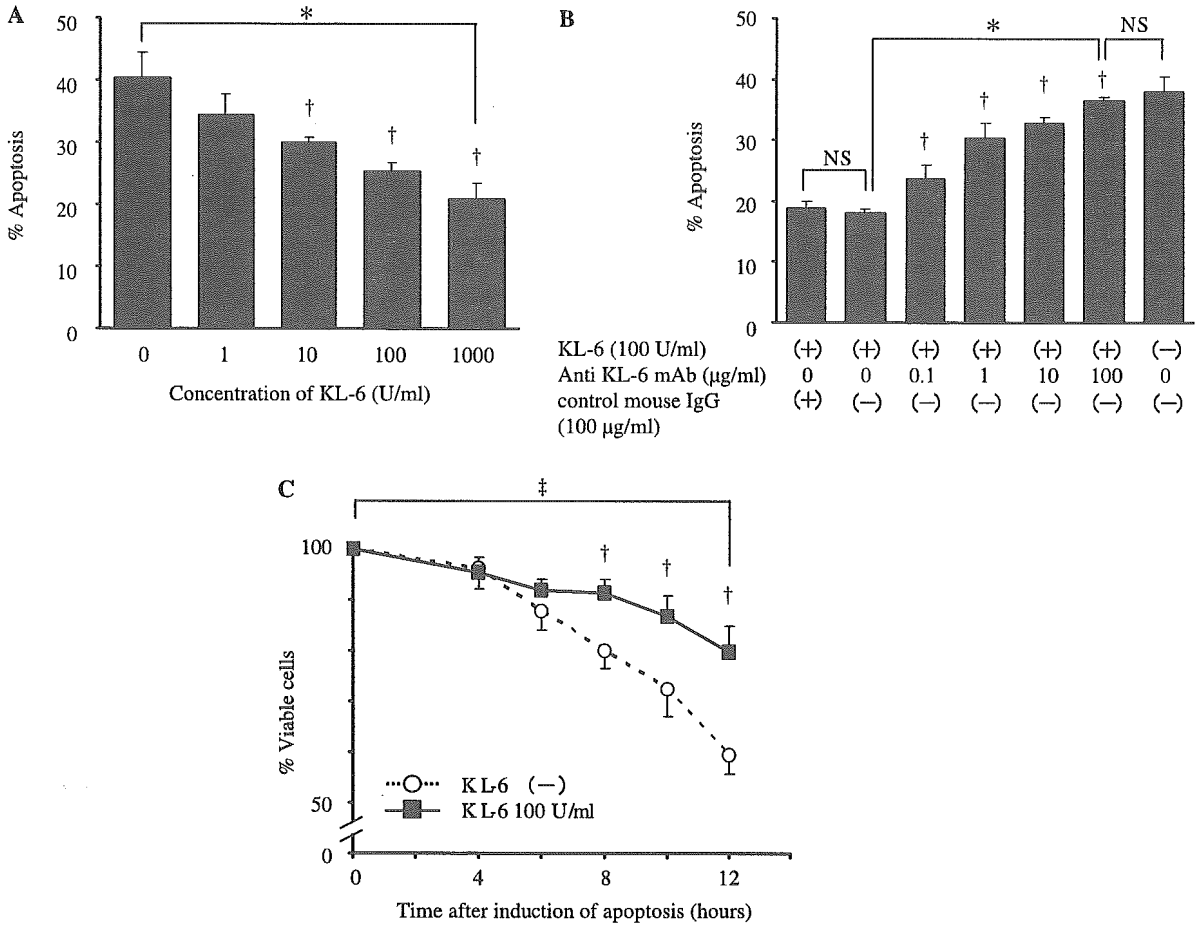

Fig. 2. Effect of KL-6 and anti-KL-6 mAb on the apoptosis of CCD-11Lu fibroblasts. Quantification of viable cells following apoptotic induction was assessed by MTS absorbance measured as described under Materials and methods. (A) Following the induction of apoptosis, more viable cells were detected with increasing concentrations of KL-6 ($^{*}P < 0.05$, one-way ANOVA). At KL-6 concentrations of 10, 100, and 1000 U/ml, the anti-apoptotic effect of KL-6 was statistically significant ($^{\dagger}P < 0.05$, Student's t test). Values are represented as the percentage of MTS absorbance relative to that from the cells without any treatment. (B) The anti-apoptotic effect of 100 U/ml of KL-6 on CCD-11Lu cells was inhibited by the addition of anti-KL-6 mAb in a dose-dependent manner ($^{*}P < 0.0001$, one-way ANOVA). The inhibitory effect obtained at anti-KL-6 mAb concentrations ranging from 0.1 to 100 μg/ml was statistically significant ($^{\dagger}P < 0.05$, Student's t test). Control mouse IgG had no effect. Values are represented as the percentage of MTS absorbance relative to that from the cells without any treatment. (C) The anti-apoptotic effect of 100 U/ml of KL-6 was observed as early as 8 h after the induction of apoptosis ($^{\dagger}P < 0.05$, Student's t test). This trend persisted until the observation was stopped 12 h after apoptotic induction ($^{\ddagger}P < 0.005$, repeated measurement of ANOVA). Data were determined in triplicate and expressed as means ± SD (A–C).

promote intraalveolar fibrosis by inducing transmigration and the accumulation of fibroblasts.

KL-6 showed a potent anti-apoptotic effect on lung fibroblasts. This result suggests that KL-6 may be involved in the survival of lung fibroblasts after apoptotic induction by the Fas–Fas ligand system. The pathogenesis of pulmonary fibrosis is now considered to be aberrant wound repair and remodeling that follows sequential lung injury [25]. Dysregulated epithelial–mesenchymal interaction is believed to promote migration and proliferation of fibroblasts, myofibroblast differentiation, and extracelluar matrix production. Another aspect of dysregulated epithelial–mesenchymal interaction is the difference in apoptotic response between AEC and fibroblasts [26]. Previous studies have shown that the Fas–Fas ligand pathway is augmented in the lung from patients with ILD [27], which induces apoptosis of AEC but not fibroblasts [28]. Anti-apoptotic proteins such as X chromosome-linked inhibitor of apoptosis (ILP) and FLICE-like inhibitor protein ($FLIP_L$) may play an important role in preventing Fas-mediated apoptosis in lung fibroblasts [28]. Nuclear factor-κB (NF-κB), a transcription factor is one of the regulators of ILP and $FLIP_L$ [29,30]. Based on these features, lung fibroblasts have an original tendency to resist Fas-mediated apoptosis compared to AEC. Our observations of a potent anti-apoptotic effect of KL-6 on lung fibroblasts indicated there is an augmentation of apoptotic tolerance to the Fas–Fas ligand system in lung fibroblasts.

We have demonstrated that the pro-proliferative and anti-apoptotic activities of purified KL-6 were comparable to those of bFGF, PDGF-BB, TFG-β_1, and -β_2 in this experimental system. Previous studies have demonstrated that proliferation in the lung microenvironment is regulated by a complex integration of a number of stimulatory factors such as bFGF [23], PDGF-BB [22], TGF-β [21], connective tissue growth factor (CTGF) [24], epidermal

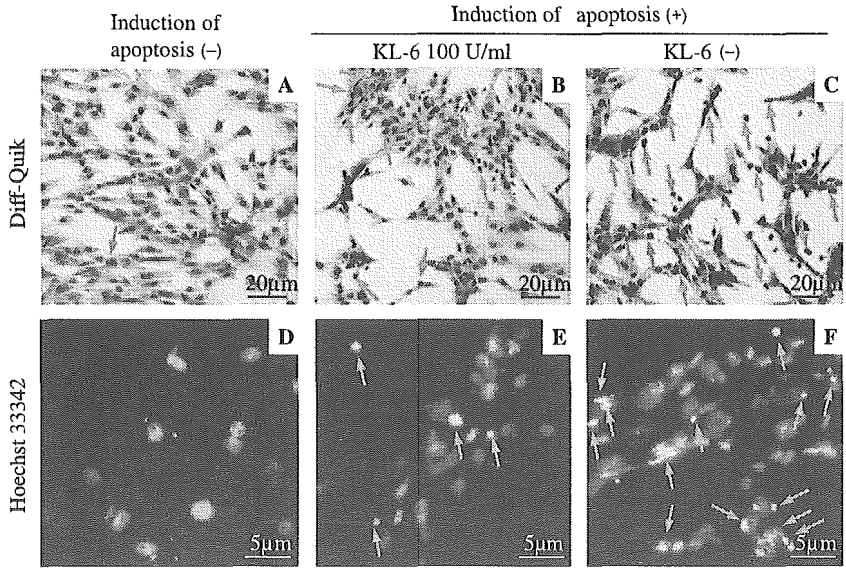

Fig. 3. Anti-apoptotic effect of KL-6 on CCD-11Lu fibroblasts assessed morphologically. CCD-11Lu incubated with or without 100 ng/ml of anti-Fas mAb and 10 μg/ml of cycloheximide for 12 h in the presence or absence of KL-6 were stained with Diff-Quik (upper panels, A–C) and Hoechst 33342 (lower panels, D–F). The left panel of each staining result (A,D) shows the cells without apoptotic induction (negative control). The middle and the right panels of each staining show the cells with apoptotic induction that were cultured in the presence (B,E) or the absence (C,F) of 100 U/ml of KL-6, respectively. Red arrows indicate apoptotic cells, which were characterized by their condensed chromatin and fragmented nuclei.

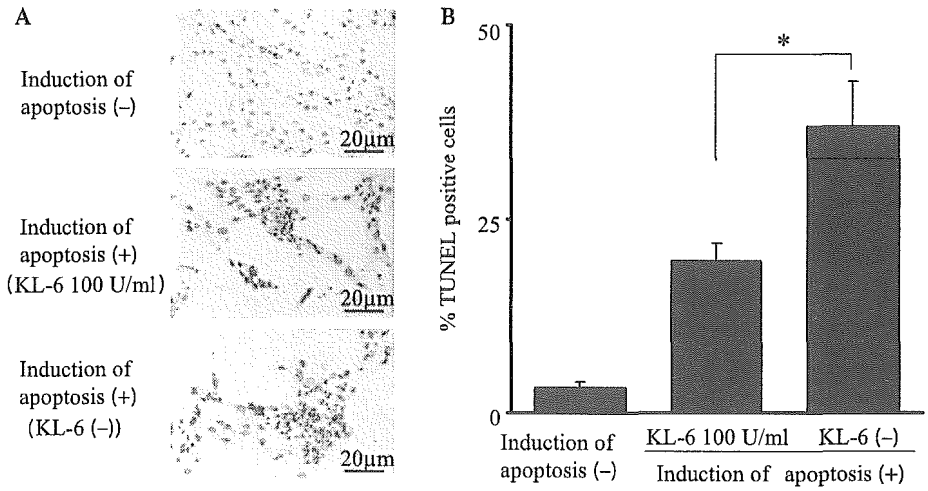

Fig. 4. The TUNEL staining of CCD-11Lu fibroblasts. (A) CCD-11Lu cultured in the presence or absence of KL-6 following apoptotic induction were stained using an In Situ Cell Death Detection kit POD. The upper panel shows the cells without apoptotic induction as a negative control. The middle and the lower panels show the cells with apoptotic induction cultured in the presence or absence of 100 U/ml of KL-6, respectively. (B) The percentages of TUNEL positive cells relative to the total cells are represented. At least 1000 cells in each sample were counted. Data were determined in triplicate and expressed as means ± SD ($^*P < 0.05$, Mann–Whitney's U test).

growth factor (EGF) [31], and interleukin-1β (IL-1β) [32]. bFGF, PDGF-BB, TFG-β_1, and -β_2 are multifunctional cytokines that are likewise involved in the suppression of apoptosis in many cell types [33–35]. Pathological investigations using lung specimens have indicated there is strong expression of these cytokines in the lungs of patients with IPF. It has also been reported that activated macrophages, fibroblasts, and AECs are the predominant sites where these cytokines are overproduced [21]. We previously showed that PDGF or FGF had no effect on chemotaxis of fibroblasts when 1000 U/ml of KL-6 was present [16]. In the present study, KL-6 had an additive promoting effect on the maximum effect of these cytokines in vitro, in terms of proliferative and anti-apoptotic activities. Taken together, these observations indicate that KL-6 is one of the most important factors for the pathogenesis of IPF.

The above findings support our hypothesis that KL-6 is one of the key molecules playing a crucial role in aberrant wound repair and remodeling. Considering the importance of KL-6 in the fibrotic process of ILD, anti-KL-6 mAb or inhibition of the receptor for the KL-6 epitope on MUC1 mucin, may indicate possible therapeutic applications for

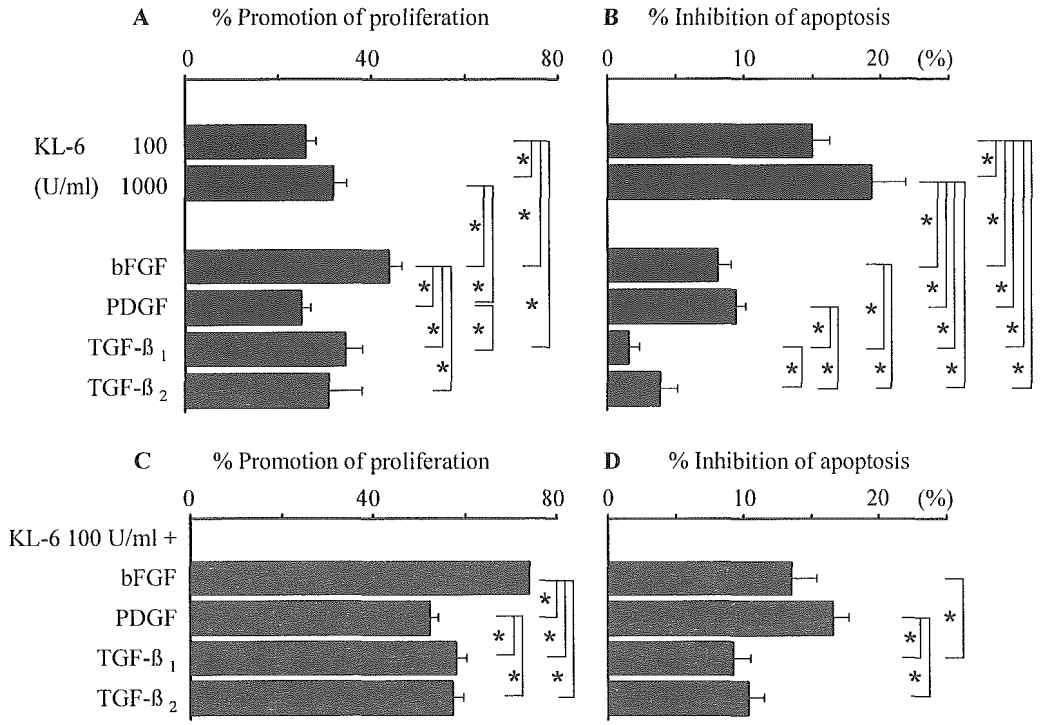

Fig. 5. Comparison of the pro-proliferative and anti-apoptotic effects of bFGF, PDGF-BB, TGF-β_1, and -β_2, with that of KL-6. (A) The relative proliferation-promoting effects of CCD-11Lu co-cultured with bFGF (100 ng/ml), PDGF-BB (20 ng/ml), TGF-β_1, -β_2 (2 ng/ml), and KL-6 (100 and 1000 U/ml) were compared with cells cultured without any cytokines. The promoting effect of bFGF was significantly stronger compared with 1000 U/ml of KL-6 (*$P < 0.05$, Student's t test). The promoting effect of PDGF-BB was comparable with that of 100 U/ml of KL-6. The promoting effects of TGF-β_1 and -β_2 were comparable with that of 1000 U/ml of KL-6. (B) The relative inhibitory effects on apoptosis of CCD-11Lu co-cultured with bFGF (100 ng/ml), PDGF-BB (20 ng/ml), TGF-β_1, and -β_2 (2 ng/ml), and KL-6 (100 and 1000 U/ml) were compared with cells cultured without any cytokines. The inhibitory effect of KL-6 was the strongest compared with those of bFGF, PDGF-BB, TGF-β_1, and -β_2 (*$P < 0.05$, Student's t test). (C,D) The additive effect of KL-6 (100 U/ml) to bFGF (100 ng/ml), PDGF-BB (20 ng/ml), TGF-β_1, and -β_2 (2 ng/ml) on the proliferation and anti-apoptosis of CCD-11Lu are demonstrated. KL-6 showed additive effects in both proliferation and anti-apoptosis that were accelerated by bFGF, PDGF-BB, TGF-β_1, and -β_2.

IPF. KL-6 failed to accelerate proliferation of murine fibroblasts, suggesting the existence of a species-specific receptor for KL-6. However, the receptor for KL-6 has not yet been identified. We have previously demonstrated that anti-KL-6 mAb counteracts the chemotaxis of KL-6 in human fibroblasts [16]. This result, along with our present results showing an inhibitory effect of the anti-KL-6 mAb against the pro-proliferative and anti-apoptotic effects of KL-6, indicate that KL-6 could be a molecular target for future treatment of ILD.

In conclusion, we have demonstrated the potent pro-proliferative and anti-apoptotic effects of KL-6 on human lung fibroblasts. These findings suggest a novel pathophysiological role for KL-6 in IPF, as it stimulates fibrotic processes in the alveolar space. In addition, the present results support our hypothesis that KL-6 is one of the key molecules involved in epithelial–mesenchymal interactions, and KL-6 appears to be a promising molecular target for the treatment of ILD.

References

[1] A.L. Katzenstein, J.L. Myers, Idiopathic pulmonary fibrosis: clinical relevance of pathologic classification, Am. J. Respir. Crit. Care Med. 157 (1998) 1301–1315.

[2] M. Selman, T.E. King, A. Pardo, Idiopathic pulmonary fibrosis: prevailing and evolving hypotheses about its pathogenesis and implications for therapy, Ann. Intern. Med. 134 (2001) 136–151.

[3] N. Kohno, M. Akiyama, S. Kyoizumi, M. Hakoda, K. Kobuke, M. Yamakido, Detection of soluble tumor-associated antigens in sera and effusions using novel monoclonal antibodies, KL-3 and KL-6, against lung adenocarcinoma, Jpn. J. Clin. Oncol. 18 (1988) 203–216.

[4] N. Kohno, Y. Inoue, H. Hamada, S. Fujioka, S. Fujino, A. Yokoyama, K. Hiwada, N. Ueda, M. Akiyama, Difference in serodiagnostic values among KL-6-associated mucins classified as cluster 9, Int. J. Cancer Suppl. 8 (1994) 81–83.

[5] N. Kohno, S. Kyoizumi, Y. Awaya, H. Fukuhara, M. Yamakido, M. Akiyama, New serum indicator of interstitial pneumonitis activity. Sialylated carbohydrate antigen KL-6, Chest 96 (1989) 68–73.

[6] N. Kohno, A. Yokoyama, Y. Hirasawa, K. Kondo, S. Fujino, M. Abe, K. Hiwada, Comparative studies of circulating KL-6, type III procollagen N-terminal peptide and type IV collagen 7S in patients with interstitial pneumonitis and alveolar pneumonia, Respir. Med. 91 (1997) 558–561.

[7] H. Ohnishi, A. Yokoyama, K. Kondo, H. Hamada, M. Abe, K. Nishimura, K. Hiwada, N. Kohno, Comparative study of KL-6, surfactant protein-A, surfactant protein-D, and monocyte chemoattractant protein-1 as serum markers for interstitial lung diseases, Am. J. Respir. Crit. Care Med. 165 (2002) 378–381.

[8] N. Kohno, Y. Awaya, T. Oyama, M. Yamakido, M. Akiyama, Y. Inoue, A. Yokoyama, H. Hamada, S. Fujioka, K. Hiwada, KL-6, a mucin-like glycoprotein, in bronchoalveolar lavage fluid from patients with interstitial lung disease, Am. Rev. Respir. Dis. 148 (1993) 637–642.

[9] A. Yokoyama, N. Kohno, H. Hamada, M. Sakatani, E. Ueda, K. Kondo, Y. Hirasawa, K. Hiwada, Circulating KL-6 predicts the outcome of rapidly progressive idiopathic pulmonary fibrosis, Am. J. Respir. Crit. Care Med. 158 (1998) 1680–1684.
[10] N. Kohno, H. Hamada, S. Fujioka, K. Hiwada, M. Yamakido, M. Akiyama, Circulating antigen KL-6 and lactate dehydrogenase for monitoring irradiated patients with lung cancer, Chest 102 (1992) 117–122.
[11] H. Ohnishi, A. Yokoyama, Y. Yasuhara, A. Watanabe, T. Naka, H. Hamada, M. Abe, K. Nishimura, J. Higaki, J. Ikezoe, N. Kohno, Circulating KL-6 levels in patients with drug induced pneumonitis, Thorax 58 (2003) 872–875.
[12] R. Janssen, H. Sato, J.C. Grutters, A. Bernard, H. van Velzen-Blad, R.M. du Bois, J.M. van den Bosch, Study of Clara cell 16, KL-6, and surfactant protein-D in serum as disease markers in pulmonary sarcoidosis, Chest 124 (2003) 2119–2125.
[13] T. Takahashi, M. Munakata, I. Suzuki, Y. Kawakami, Serum and bronchoalveolar fluid KL-6 levels in patients with pulmonary alveolar proteinosis, Am. J. Respir. Crit. Care Med. 158 (1998) 1294–1298.
[14] A. Ishizaka, T. Matsuda, K.H. Albertine, H. Koh, S. Tasaka, N. Hasegawa, N. Kohno, T. Kotani, H. Morisaki, J. Takeda, M. Nakamura, X. Fang, T.R. Martin, M.A. Matthay, S. Hashimoto, Elevation of KL-6, a lung epithelial cell marker, in plasma and epithelial lining fluid in acute respiratory distress syndrome, Am. J. Physiol. Lung Cell. Mol. Physiol. 286 (2004) L1088–L1094.
[15] H. Hamada, N. Kohno, A. Yokoyama, Y. Hirasawa, K. Hiwada, M. Sakatani, E. Ueda, KL-6 as a serologic indicator of *Pneumocystis carinii* pneumonia in immunocompromised hosts, Intern. Med. 37 (1998) 307–310.
[16] Y. Hirasawa, N. Kohno, A. Yokoyama, Y. Inoue, M. Abe, K. Hiwada, KL-6, a human MUC1 mucin, is chemotactic for human fibroblasts, Am. J. Respir. Cell. Mol. Biol. 17 (1997) 501–507.
[17] H. Hamada, N. Kohno, K. Hiwada, A new serum tumor marker, CAM 123-6, highly specific to pulmonary adenocarcinoma, Jpn. J. Cancer Res. 85 (1994) 211–219.
[18] S.K. Goparaju, P.S. Jolly, K.R. Watterson, M. Bektas, S. Alvarez, S. Sarkar, L. Mel, I. Ishii, J. Chun, S. Milstien, S. Spiegel, The S1P2 receptor negatively regulates platelet-derived growth factor-induced motility and proliferation, Mol. Cell. Biol. 25 (2005) 4237–4249.
[19] Y. Aono, Y. Nishioka, M. Inayama, M. Ugai, J. Kishi, H. Uehara, K. Izumi, S. Sone, Imatinib as a novel antifibrotic agent in bleomycin-induced pulmonary fibrosis in mice, Am. J. Respir. Crit. Care Med. 171 (2005) 1279–1285.
[20] Y. Zhao, S.L. Young, Requirement of transforming growth factor-beta (TGF-beta) type II receptor for TGF-beta-induced proliferation and growth inhibition, J. Biol. Chem. 271 (1996) 2369–2372.
[21] T.A. Wynn, Fibrotic disease and the T(H)1/T(H)2 paradigm, Nat. Rev. Immunol. 4 (2004) 583–594.
[22] A. Abdollahi, M. Li, G. Ping, C. Plathow, S. Domhan, F. Kiessling, L.B. Lee, G. McMahon, H.J. Grone, K.E. Lipson, P.E. Huber, Inhibition of platelet-derived growth factor signaling attenuates pulmonary fibrosis, J. Exp. Med. 201 (2005) 925–935.
[23] V.C. Midgley, L.M. Khachigian, Fibroblast growth factor-2 induction of platelet-derived growth factor-C chain transcription in vascular smooth muscle cells is ERK-dependent but not JNK-dependent and mediated by Egr-1, J. Biol. Chem. 279 (2004) 40289–40295.
[24] S.H. Wu, X.H. Wu, C. Lu, L. Dong, Z.Q. Chen, Lipoxin A4 inhibits proliferation of human lung fibroblasts induced by CTGF, Am. J. Respir. Cell. Mol. Biol. (2005), [Epub ahead of print].
[25] M. Selman, A. Pardo, The epithelial/fibroblastic pathway in the pathogenesis of idiopathic pulmonary fibrosis, Am. J. Respir. Cell. Mol. Biol. 29 (2003) S93–S97.
[26] J.V. Barbas-Filho, M.A. Ferreira, A. Sesso, R.A. Kairalla, C.R. Carvalho, V.L. Capelozzi, Evidence of type II pneumocyte apoptosis in the pathogenesis of idiopathic pulmonary fibrosis (IFP)/usual interstitial pneumonia (UIP), J. Clin. Pathol. 54 (2001) 132–138.
[27] K. Kuwano, H. Miyazaki, N. Hagimoto, M. Kawasaki, M. Fujita, R. Kunitake, Y. Kaneko, N. Hara, The involvement of Fas–Fas ligand pathway in fibrosing lung diseases, Am. J. Respir. Cell. Mol. Biol. 20 (1999) 53–60.
[28] T. Tanaka, M. Yoshimi, T. Maeyama, N. Hagimoto, K. Kuwano, N. Hara, Resistance to Fas-mediated apoptosis in human lung fibroblast, Eur. Respir. J. 20 (2002) 359–368.
[29] S. Bai, H. Liu, K.H. Chen, P. Eksarko, H. Perlman, T.L. Moore, R.M. Pope, NF-kappaB-regulated expression of cellular FLIP protects rheumatoid arthritis synovial fibroblasts from tumor necrosis factor alpha-mediated apoptosis, Arthritis Rheum. 50 (2004) 3844–3855.
[30] Z. Li, J. Zhang, D. Chen, H.B. Shu, Casper/c-FLIP is physically and functionally associated with NF-kappaB1 p105, Biochem. Biophys. Res. Commun. 309 (2003) 980–985.
[31] M.P. Chong, G.J. Barritt, M.F. Crouch, Insulin potentiates EGFR activation and signaling in fibroblasts, Biochem. Biophys. Res. Commun. 322 (2004) 535–541.
[32] J.L. Ingram, A.B. Rice, K. Geisenhoffer, D.K. Madtes, J.C. Bonner, IL-13 and IL-1beta promote lung fibroblast growth through coordinated up-regulation of PDGF-AA and PDGF-Ralpha, FASEB J. 18 (2004) 1132–1134.
[33] E.A. Harrington, M.R. Bennett, A. Fanidi, G.I. Evan, c-Myc-induced apoptosis in fibroblasts is inhibited by specific cytokines, EMBO J. 13 (1994) 3286–3295.
[34] H. Kazama, S. Yonehara, Oncogenic K-Ras and basic fibroblast growth factor prevent Fas-mediated apoptosis in fibroblasts through activation of mitogen-activated protein kinase, J. Cell Biol. 148 (2000) 557–566.
[35] H.H. Chen, S. Zhao, J.G. Song, TGF-beta1 suppresses apoptosis via differential regulation of MAP kinases and ceramide production, Cell Death Differ. 10 (2003) 516–527.

Identification of Serum Proteins Related to Adverse Effects Induced by Docetaxel Infusion from Protein Expression Profiles of Serum Using SELDI ProteinChip System

YUJI HEIKE[1,2,3], MAMI HOSOKAWA[1,2], SHOZO OSUMI[1], DAISUKE FUJII[1], KENJIRO AOGI[1], NAGIO TAKIGAWA[1], MIKIKO IDA[1], HISAO TAJIRI[1], KENJI EGUCHI[1], MIEKO SHIWA[4], RUMI WAKATABE[4], HISASHI ARIKUNI[5], YOICHI TAKAUE[2] and SHIGEMITSU TAKASHIMA[1]

[1]*Department of Medical Oncology and Clinical Research, National Shikoku Cancer Center, 13-Horinouchi, Matsuyama, Ehime 790-0007;*
[2]*Hematopoietic Stem Cell Transplant/Immunotherapy Unit, National Cancer Center Hospital, Tsukiji, Chuo-ku, Tokyo 104-0045;*
[3]*Pharmacology Division, National Cancer Center Research Insitute, 5-1-1, Tsukiji, Chuo-ku, Tokyo 104-0045;*
[4]*Ciphergen Biosystems K.K., Yokohama Business Park Hi-tech Center 1F, 134 Godo-cho, Hodogaya-ku, Yokohama-shi, Kanagawa, 240-0005;*
[5]*Sumitomo-Bioscience, Yokohama Business Park Hi-tech Center 1F, 134 Godo-cho, Hodogaya-ku, Yokohama-shi, Kanagawa, 240-0005, Japan*

Abstract. *Background: For the development of quick and easy methods for screening and identifying treatment-responsive proteins, we determined the protein expression profile of the serum after docetaxel infusion using a surface-enhanced laser desorption/ionization time-of-flight mass spectroscopy (SELDI TOF-MS) system. Materials and Methods: Blood from breast cancer patients was collected before and 4, 8, 24 and 48 hours after docetaxel infusion. The protein expression profile was determined by a SELDI TOF-MS system. The relative expression levels of target proteins were compared during the time-course after docetaxel injection. Results: We identified two representative proteins with molecular weights of 7790 Da and 9285 Da. The 7790 Da protein was high molecular weight kininogen, and the 9285 Da protein was apolipoprotein A-II. These two proteins had similar expression patterns in 5 patients, except one patient who experienced severe, acute, adverse effects. Conclusion: These results suggest that protein expression profiles determined by SELDI TOF-MS represent useful data for the identification of treatment-responsive proteins.*

Correspondence to: Yuji Heike, MD, PhD, Pharmacology Division, National Cancer Center Research Insitute, 5-1-1, Tsukiji, Chuo-ku, Tokyo 104-0045, Japan. Tel: +81-3-3542-2511, Fax: +81-3-3547-5228, e-mail: yheike@ncc.go.jp

Key Words: SELDI TOF-MS, protein expression profile, adverse effect, ProteinChip System, HMW kininogen, apolipoprotein A-II.

Docetaxel is a key drug used to treat breast cancer. As docetaxel is hydrophobic, polysorbate 80 and ethanol are used as solvents. Some patients experience acute adverse effects, including anaphylactoid reactions, during docetaxel infusion and may develop shock. Several reports suggest that these adverse effects are caused by the solvent, which contains polysorbate 80 (1, 2). However, the mechanisms of these adverse effects are unknown. One approach to determine the mechanisms causing adverse effects is to analyze the treatment-responsive proteins.

Pharmacokinetics and pharmacodynamics are important areas of research in clinical pharmacology that analyze drug metabolism and host responses in order to predict the response and adverse effects of treatment.

Recently, DNA chip technology, such as DNA microarrays and cDNA arrays, has been used to predict responses to treatment. Some promising results have been reported in studies of irinotecan and other drugs (3-5), and there is no doubt that this genetic approach could be used to predict the potential response of a patient to treatment. However, genetic information alone cannot perfectly predict responses to treatment, because genes do not act by themselves. Genes exert their effect through proteins after transcription and translation. Thus, protein analysis is important to predict responses to treatment.

Until recently, no ideal tools have been available to determine protein expression profiles. Although two-dimensional electrophoresis could be used for this purpose, it is labor-intensive and is not capable of high-throughput

0250-7005/2005 $2.00+.40

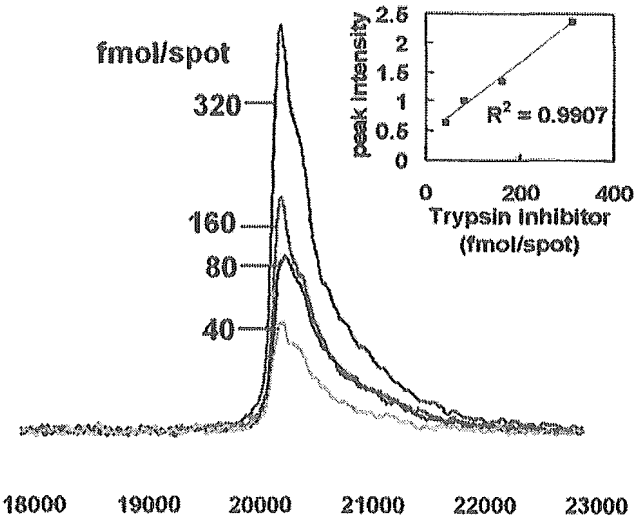

Figure 1. *Quantitative analysis. Various concentrations of trypsin inhibitor were studied with the SAX-2 (strong anion exchange) chip. Peak heights of trypsin inhibitor (molecular weight, approximately 20,000 Da) were clearly dose-dependent. The correlation coefficient calculated by Excel 2000 software was 0.99.*

analysis. Recent developments in mass spectrometry have been revolutionary in proteomic research. These new techniques are highly sensitive and have potential for various applications. Surface-enhanced laser desorption/ionization time-of-flight mass spectroscopy (SELDI TOF-MS) can be used to produce protein expression profiles. This system comprises ProteinChip arrays and time-of-flight mass spectrometry (TOF-MS). ProteinChip arrays possess varying chromatographic properties, such as anion exchange, cation exchange, metal affinity and reverse phase. The combination of the type of chip array and the washing conditions, such as the pH or salt concentration in the buffer, allows rapid analysis of protein profiles with only a small amount of sample. In the present study, we used the SELDI TOF-MS system to find docetaxel treatment-responsive proteins.

To select treatment-responsive proteins, it was necessary to compare the protein expression levels at several time-points after the treatment. However, no previous studies have indicated that mass spectrometry can be used for quantitative analysis of proteins. In the present study, we conducted a quantitative analysis of the targeted proteins. After selecting two representative treatment-responsive proteins, we used SELDI TOF-MS to determine the conditions for column purification of the proteins. We then determined the amino acid sequence of the purified proteins. The relationship between these proteins and docetaxel-induced shock is discussed, as well as the usefulness of the present approach in clinical pharmacology and clinical proteomics.

Table I.

Research ID	Gender	Protocol	Acute response
A	F	tri-week (60mg/m^2)	No
B	F	tri-week (60mg/m^2)	No
C	F	tri-week (60mg/m^2)	No
D	F	tri-week (60mg/m^2)	Shock
E	F	weekly (40mg/m^2)	No

Materials and Methods

Quantitative analysis. Various concentrations of trypsin inhibitor (Sigma-Aldrich, St. Louis, MO, USA) were studied using the SAX-2 chip (Ciphergen Biosystems, Fremont, CA, USA), and the heights of peaks were compared for the quantitative analysis.

Patients and blood samples. Ten breast cancer patients receiving docetaxel treatment were enrolled in this experiment, after providing informed consent in accordance with the guidelines of the National Shikoku Cancer Center Institutional Review Board, Japan. The results from 6 representative patients are described in the present report. Patients receiving docetaxel injections (60 mg/m^2) every 3 weeks and patients receiving weekly docetaxel injections (40 mg/m^2) were enrolled in this study. Dexamethasone (8 mg) was used as a premedication 30 min prior to docetaxel infusion. Docetaxel was administered as a 30-min infusion for patients on the weekly schedule and as a 60-min infusion for patients on the 3-week schedule. After the docetaxel infusions, oral dexamethasone (4 mg) was taken twice daily for one day for patients on the weekly schedule and for 2 days for patients on the 3-week schedule.

Blood (5 ml) was collected before docetaxel infusion and 4, 8, 24 and 48 h after docetaxel infusion. Serum was prepared quickly and stored at -80°C until analysis.

Medical information, such as adverse effects after docetaxel injection, was obtained from the medical records and entered into a database in accordance with the privacy policy of our institution.

Protein expression profiles. Protein expression profiles were determined using a SELDI TOF-MS system (Ciphergen Biosystems). IMAC3 (immobilized metal affinity capture), WCX-2 (weak cation exchange) and SAX-2 (strong anion exchange) ProteinChip arrays were used for analysis. The serum samples were centrifuged at 12,000 rpm using a microcentrifuge (TOMY Tech USA, Fremont, CA, USA). The supernatant was vigorously mixed with urea buffer (8 M urea:1% CHAPS/PBS, 1:1) for 10 min at 4°C and was diluted with $^{5x}_{1x}$ volumes of binding buffer (PBS for IMAC3, 50 mM phosphate buffer (pH 6) for WCX-2 and 50 mM Tris-HCl (pH 8) for SAX-2).

To immobilize copper onto the IMAC3 surface, 5 μl of 50 mM copper sulfate was loaded, and the chip was shaken for 5 min. Excess copper was removed under running deionized water, and the chip was shaken for 5 min with 10 μl of 50 mM sodium acetate (pH 4). The chip was rinsed under running deionized water and was then ready to be used for the analysis step.

The following procedure was used for chip analysis: (i) each spot was equilibrated with 150 μl of binding buffer twice on a shaker for 5 min, and excess buffer was removed; (ii) diluted samples (50 μl per

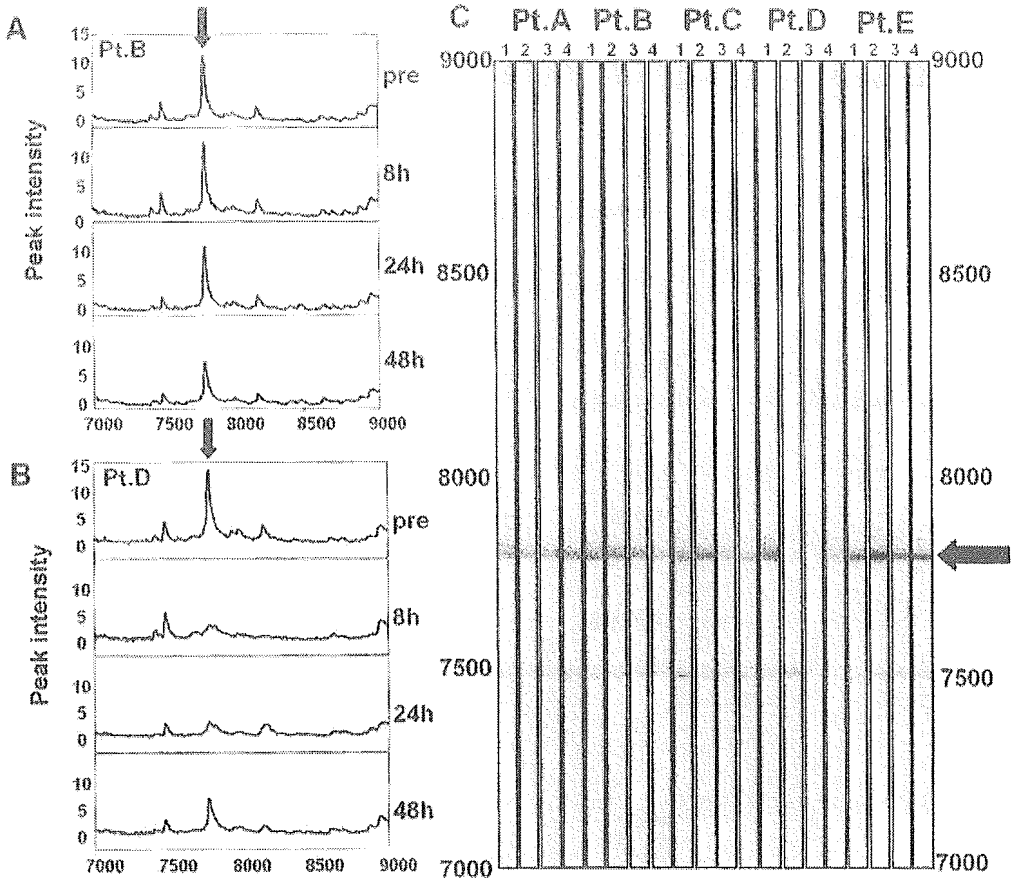

Figure 2. *Expression of 7790 Da protein at different times. (A) Typical response pattern of the 7790 Da protein in patient B, in trace view. (B) Specific response pattern in patient D, in trace view. (C) Gel view of 5 samples (Pt. A-Pt. E). Lane 1, pre-injection; lane 2, 8 h after injection; lane 3, 24 h after injection; and lane 4, 48 h after injection. In patient D, the protein suddenly disappeared and slowly reappeared over a period of days.*

spot) were loaded, and the chip was incubated on a shaker for 20 min at room temperature; (iii) the chip was washed 3 times with 150 μl per spot of binding buffer; (iv) the chip was rinsed with distilled water and dried; and (v) each spot was treated with 0.5 μl of saturated sinapinic acid prepared in aqueous solution containing 50% acetonitrile and 0.5% trifluoroacetic acid. Captured proteins were directly detected using a PBS II ProteinChip Reader (Ciphergen Biosystems).

Screening of docetaxel-responsive proteins. Quantitative analysis of proteins was performed using Peaks 3.0 software (Ciphergen Biosystems). Expression levels of the proteins were compared over the time-course of the experiment. Two representative proteins, that had similar expression patterns in patients, were selected.

Protein purification and amino acid sequencing. To determine the optimal pH and salt concentration of the buffer for purification of the target proteins, IMAC3, WCX-2 and SAX-2 assays were performed. The target proteins were fractionated by CM Sepharose Fast Flow (Amersham Biosciences, Piscataway, NJ, USA) and separated by 16% SDS polyacrylamide gel electrophoresis using the method reported by Schagger and Jagow (6). Electroblotting to PVDF membrane was performed using a TEFCO electroblotting system (TEFCO. Co., Ltd., Tokyo, Japan). Amino acid sequences of the purified proteins were analyzed according to the Edman method using a Procise 494 HT Protein Sequencing System (Applied Biosystems, Foster City, CA, USA). Database searches of the sequence data were performed using SWISS-PROT.

Results

Quantitative analysis. To confirm that the SELDI TOF-MS system can be used for quantitative analysis, various concentrations of trypsin inhibitor were analyzed using the SAX-2 chip. The peak heights of trypsin inhibitor (molecular weight, approximately 20,000 Da) occurred in a dose-dependent manner (Figure 1) with a correlation coefficient of 0.99 calculated by Excel 2000 software. The SELDI TOF-MS system can therefore be used to quantitatively analyze protein profiles.

Patient characteristics and acute reaction related to docetaxel injection. Ten patients were enrolled in the study, and the data from 6 representative patients are presented in this report. The background of the patients, injection schedule and acute reactions recorded in the medical records are

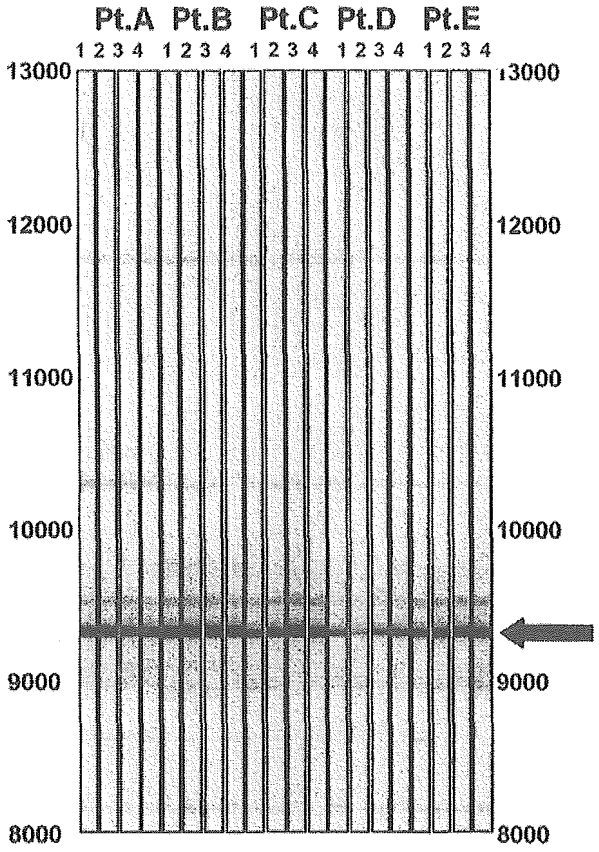

Figure 3. *Gel view of 9285 Da protein in 5 patients. In patient D, expression of the 9285 Da protein decreased transiently. The expression of this protein was unchanged in all other patients. Lane 1, pre-injection; lane 2, 8 h after injection; lane 3, 24 h after injection; and lane 4, 48 h after injection.*

summarized in Table I. Five of the 6 patients experienced no severe adverse effects, although slight flushing of the face was observed in two patients. Only one patient (patient D) experienced severe, acute, adverse effects and experienced signs and symptoms of shock. Severe flushing of the face, tachypnea with dyspnea, tachycardia and low blood pressure were observed in patient D. The docetaxel injection was stopped immediately and additional dexamethasone (8 mg) was injected. The patient recovered from shock, and docetaxel dissolved in simple saline (without polysorbate 80) was slowly infused. The infusion was completed without any additional adverse effects.

Protein profiles and docetaxel-responsive proteins. We compared serial profiles from the same patients according to the time-course of the infusion and selected two peaks of interest. The peaks occurred at 7790 Da and 9285 Da. Figure 2A shows data from patient B, and Figure 2B shows data from patient D. Figure 2C shows data from 5 patients and indicates that the expression of the 7790 Da protein disappeared suddenly only in patient D. Patient D, who

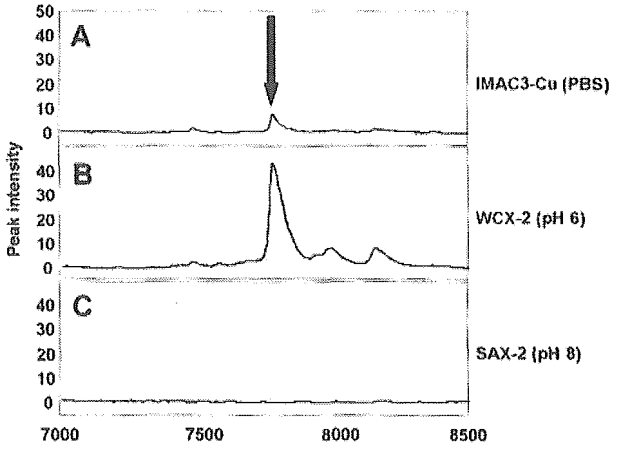

Figure 4. *Binding capacity of 7790 Da protein to three different chips. (A) Immobilized metal affinity capture using copper (IMAC3-Cu chip, PBS buffer), (B) weak cation exchange (WCX-2 chip, pH 6 buffer) and (C) strong anion exchange (SAX-2 chip, pH 8 buffer). The signal obtained from the WCX-2 chip displayed the highest intensity.*

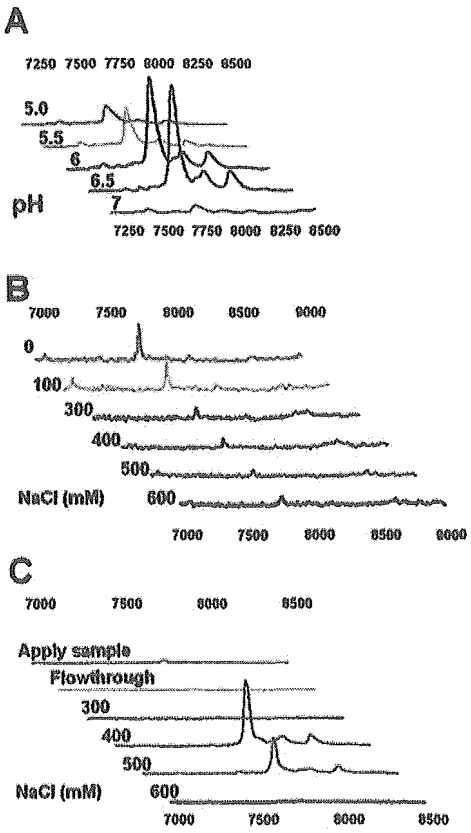

Figure 5. *Capture and elution conditions for 7790 Da protein. (A) Capture pH for the 7790 Da protein using the WCX-2 chip. (B) NaCl concentration for elution of the 7790 Da protein from the WCX-2 chip. (C) NaCl concentration for purification of the 7790 Da protein by CM sepharose affinity chromatography. These results suggest that the best conditions were pH 6 for capture and 300-400 mM NaCl for elution from the WCX-2 chip. In CM sepharose columns, buffer at pH 6 was used as a capture solution, and the optimal concentration of NaCl for elution was 400 mM.*

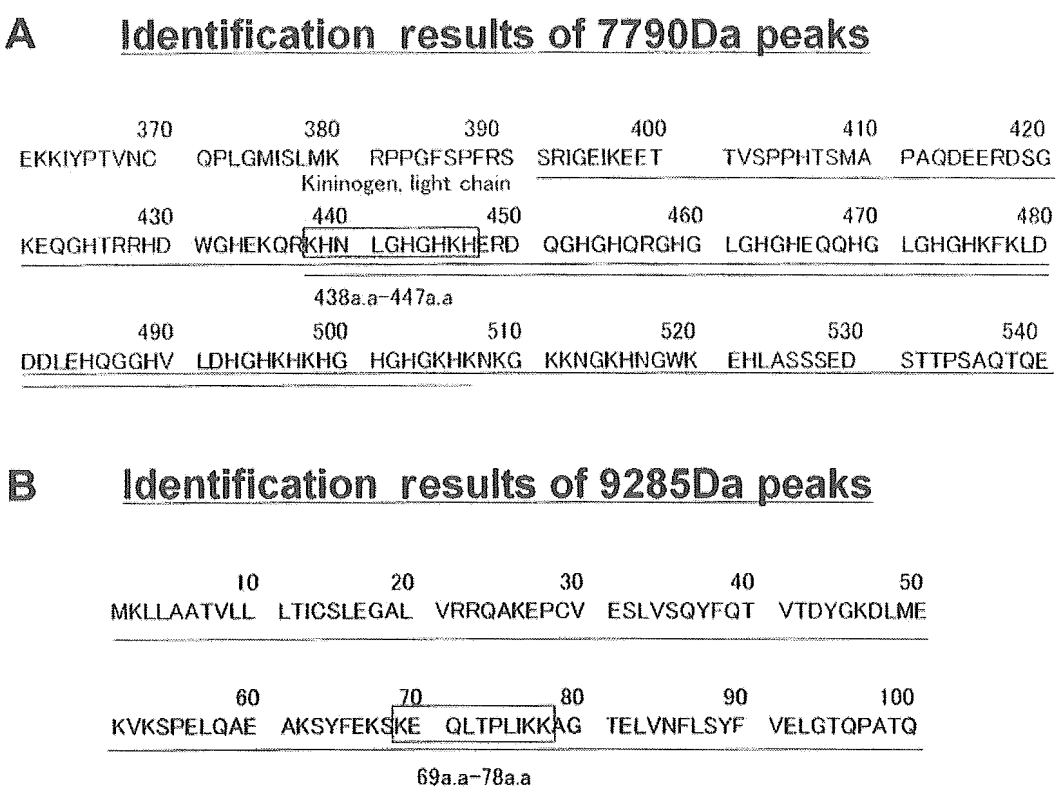

Figure 6. *Amino acid sequences of target proteins. (A) Ten amino acids from the NH3 terminal of the 7790 Da protein were analyzed according to the Edman method. The sequence was identical to amino acids 438-447 of high molecular weight kininogen. (B) Ten amino acids from a fragment of the 9285 Da protein were analyzed after in-gel digestion. The sequence was identical to amino acids 69-78 of apolipoprotein A-II.*

experienced severe adverse effects during docetaxel injection, displayed a rapid down-regulation of the 7790 Da protein, but the expression of this protein recovered over several days. Figure 3 shows gel view data of the 9285 Da protein from the same samples. The expression pattern of this protein was almost the same as the 7790 Da protein.

Purification of target proteins. To establish a procedure to purify the target proteins, we determined which chip is preferable to capture the target proteins, and then determined the optimal pH and salt concentration in the buffer using protein arrays. The results revealed that both proteins bound to the WCX-2 chip more strongly than to the other two chips (data from 7790 Da protein shown in Figure 4).

The capture pH and the NaCl concentration for elution of the 7790 Da protein were investigated using the WCX-2 chip (Figure 5). The results indicated that the best conditions were pH 6 for capture (Figure 5A) and 300-400 mM NaCl for elution (Figure 5B). We used these conditions in large-scale purification using CM sepharose column chromatography. We diluted 11.4 ml of serum to 100 ml with sodium phosphate and citrate buffer (pH 6) and applied it to a CM sepharose column (25 cm). After equilibrating with the same buffer, elution was performed using 300-600 mM NaCl stepwise. The target protein was eluted under the conditions indicated by the protein chip analysis (Figure 5C). After the 300-400 mM NaCl fraction had been dialyzed and concentrated, the sample was applied to SDS PAGE. The band containing the 7790 Da protein was removed from the gel. The purification procedure for the 9285 Da protein was determined by almost the same process, and the protein was purified (data not shown).

Amino acid sequencing of the target proteins. To determine the amino acid sequence of the target proteins, the proteins were transferred from a gel to PVDF membranes. The amino acid sequence of the purified protein was determined according to the Edman method. A sequence of 10 amino acids from the NH3 end of the 7790 Da protein was directly analyzed and determined to be identical to amino acids 438-447 of high molecular weight (HMW) kininogen (Figure 6A). This protein was also analyzed by simple MS and MSMS system, and was identified as kininogen (Figure 7). The amino terminal end of the 9285 Da protein was blocked and could not be analyzed directly. Analysis of the amino acid sequence was therefore performed after tryptic digestion, and a 10 amino acid internal sequence from the

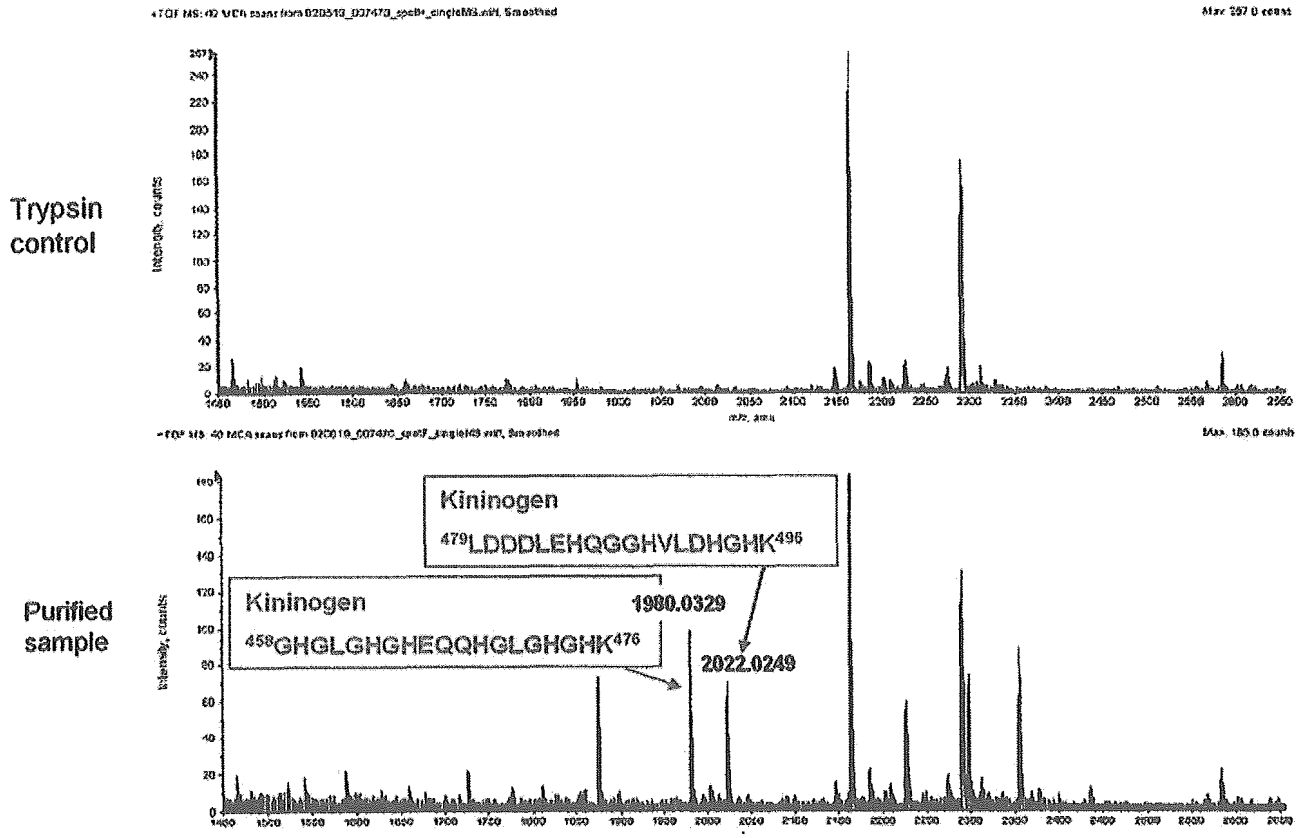

Figure 7. *Single MS and MSMS analysis of tryptic in-gel digestion sample. A piece of the gel containing 7790 Da proteins was treated with trypsin and the digested peptides were analyzed by MS and MSMS systems. Typical signals, which were considered to be fragments of kininogen, were detected.*

9285 Da protein was determined. The sequence was identical to amino acids 69-78 of apolipoprotein A-II (Figure 6B).

Discussion

Widespread expression analysis of DNA became available with the development of cDNA microarrays. Predictions of response and adverse effects were recently studied using DNA microarrays and cDNA expression arrays. However, it is clear that DNA and mRNA do not work by themselves, because mRNA must be translated into protein. This principle indicates the importance of protein analysis in post-genome projects. However, no ideal tool was previously available to determine protein expression profiles. Although two-dimensional electrophoresis could be used in this respect, the process is labor intensive and incapable of high-throughput analysis. In addition, two-dimensional electrophoresis requires skillful techniques to obtain reproducible data.

Mass spectrometry techniques have recently been used in the field of protein analysis. Liquid chromatography combined with TOF-MS offers very high sensitivity. However, this system cannot produce protein expression profiles. SELDI TOF-MS, which was recently developed, can determine protein expression profiles from crude samples, such as serum, urine and other body fluids. SELDI TOF-MS is constructed with TOF-MS and chip arrays, which have chromatographic properties on their surface. SELDI TOF-MS can be used to quickly develop protein profiles using only a small amount of sample. Several groups have found biological markers such as tumor markers using this system (7-13).

In the present study, we developed protein expression profiles from serum collected before and after docetaxel injection. We compared the protein expression profiles over the time-course of the infusion to find docetaxel-responsive proteins. We determined the amino acid sequences of the selected proteins. One of the docetaxel-responsive proteins was HMW kininogen, which is a factor in the kinin/kallikrein cascade of blood coagulation. This protein suddenly decreased in patient D, who experienced severe shock during docetaxel injection. No other patients displayed sudden decreases in this protein. Cochrane *et al.* reported a relationship between HMW kininogen and hypotensive shock (14), and Gallimore reported changes in HMW kininogen during lethal endotoxin shock (15). These reports suggest that HMW kininogen is a shock-related protein, although no previous reports have suggested that HMW kininogen is related to drug-induced

shock. The other docetaxel-responsive protein that we detected was apolipoprotein A-II, which is related to lipid and cholesterol metabolism. To the best of our knowledge, no previous reports have described an association between apolipoprotein A-II and shock.

The expression levels of HMW kininogen and apolipoprotein A-II in all patients (except for patient D) were unchanged or were slightly decreased and recovered quickly without treatment. No severe adverse effects were observed in these patients, although some experienced slight flushing of the face. These findings suggest that the homeostatic mechanisms of the body worked quickly, allowing these patients to recover from the effects of docetaxel infusion.

The roles of the proteins detected in our study in docetaxel-induced shock are unknown. Even if the changes in these proteins are the result of shock, rather than the cause of shock, this information may help elucidate the mechanisms of docetaxel-induced shock and may lead to measures for prediction of and protection from shock. Our ultimate goals are to find predictive markers for adverse effects in order to prevent/treat adverse effects, and to find molecular targets of the response. We have started to screen other proteins that respond to docetaxel treatment in order to identify proteins causing adverse effects.

Two noteworthy technical points from our experiments have not previously been reported. The first point is that we successfully used SELDI TOF-MS to compare protein expression levels in crude samples, which is an important step for screening responsive proteins. Previously, clear evidence that mass spectrometry can be used for quantitative analysis of protein from crude samples has been unavailable. Therefore, the SELDI ProteinChip System may be a key technology for protein expression analysis. The ProteinChip System can also perform high-throughput analysis. This technology is very useful for the discovery of biomarkers, particularly when a large number of samples need to be analyzed. The second noteworthy technical point is that we determined the procedure for protein purification in only one day using SELDI TOF-MS. The purification conditions determined by SELDI TOF-MS could be applied to large-scale column chromatography for both proteins. These results indicate that high-speed purification is possible using SELDI TOF-MS.

In conclusion, we found that the SELDI TOF-MS ProteinChip System can be used to compare protein expression levels in protein profiles and to quickly purify target proteins. These two points may lead to breakthroughs in clinical proteomics and clinical pharmacology.

Acknowledgements

This work was supported by grants from the Institute for Clinical Research, Department of National Hospitals, Ministry of Health, Labour and Welfare of Japan.

References

1 Rhodes A, Eastwood JB and Smith SA: Early acute hepatitis with parenteral amiodarone: a toxic effect of the vehicle? Gut *34*: 565-566, 1993.
2 Battafarano DF, Zimmerman GC, Older SA, Keeling JH and Burris HA: Docetaxel (Taxotere) associated scleroderma-like changes of the lower extremities. A report of three cases. Cancer *76*: 110-115, 1995.
3 Ando Y, Saka H, Ando M, Sawa T, Muro K, Ueoka H, Yokoyama A, Saitoh S, Shimokata K and Hasegawa Y: Polymorphisms of UDP-glucuronosyltransferase gene and irinotecan toxicity: a pharmacogenetic analysis. Cancer Res *60*: 6921-6926, 2000.
4 Ando Y, Ueoka H, Sugiyama T, Ichiki M, Shimokata K and Hasegawa Y: Polymorphisms of UDP-glucuronosyltransferase and pharmacokinetics of irinotecan. Ther Drug Monit *24*: 111-116, 2002.
5 Ando M, Ando Y, Sekido Y, Shimokata K and Hasegawa Y: Genetic polymorphisms of the UDP-glucuronosyltransferase 1A7 gene and irinotecan toxicity in Japanese cancer patients. Jpn J Cancer Res *93*: 591-597, 2002.
6 Schagger H and von Jagow G: Tricine-sodium dodecyl sulfate-polyacrylamide gel electrophoresis for the separation of proteins in the range from 1 to 100 kDa. Anal Biochem *166*: 368-379, 1987.
7 Davies H, Lomas L and Austen B: Profiling of amyloid beta peptide variants using SELDI Protein Chip arrays. Biotechniques *27*: 1258-1261, 1999.
8 Paweletz CP, Trock B, Pennanen M, Tsangaris T, Magnant C, Liotta LA and Petricoin EF 3rd: Proteomic patterns of nipple aspirate fluids obtained by SELDI-TOF: potential for new biomarkers to aid in the diagnosis of breast cancer. Disease Markers *17*: 301-307, 2001.
9 Rubin RB and Merchant M: A rapid protein profiling system that speeds study of cancer and other diseases. Am Clin Lab *19*: 28-29, 2000.
10 Verma M, Wright GLJ, Hanash SM, Gopal-Srivastava R and Srivastava S: Proteomic approaches within the NCI early detection research network for the discovery and identification of cancer biomarkers. Ann NY Acad Sci *945*: 103-115, 2001.
11 Ardekani AM, Liotta LA and Petricoin EF 3rd: Clinical potential of proteomics in the diagnosis of ovarian cancer. Expert Rev Mol Diagn *2*: 312-320, 2002.
12 Issaq HJ, Veenstra TD, Conrads TP and Felschow D: The SELDI-TOF MS approach to proteomics: protein profiling and biomarker identification. Biochem Biophys Res Commun *292*: 587-592, 2002.
13 Diamandis EP: Proteomic patterns in serum and identification of ovarian cancer. Lancet *360*: 170-171, 2002.
14 Cochrane CG and Revak SD: The participation of high molecular weight kininogen in hypotensive shock and intravascular coagulation. Clin Immunol Immunopathol *15*: 367-374, 1980.
15 Gallimore MJ, Aasen AO and Amundsen E: Changes in plasma levels of prekallikrein, kallikrein, high molecular weight kininogen and kallikrein inhibitors during lethal endotoxin shock in dogs. Haemostasis *7*: 79-84, 1987.

Received August 9, 2004
Accepted January 27, 2005

Expansion of α-Galactosylceramide-Stimulated Vα24+ NKT Cells Cultured in the Absence of Animal Materials

Yukie Harada, Osamu Imataki,† Yuji Heike,*† Hiroyuki Kawai,‡ Akihiro Shimosaka,‡ Shin-ichiro Mori,* Masahiro Kami,* Ryuji Tanosaki,* Yoshinori Ikarashi,† Akira Iizuka,* Mitsuji Yoshida,† Hiro Wakasugi,† Shigeru Saito,§ Yoichi Takaue,* Masao Takei,*‡ and Tadao Kakizoe‖*

Summary: Vα24+ NKT is an innate lymphocyte with potential antitumor activity. Clinical applications of Vα24+ natural killer (NK) T cells, which are innate lymphocytes with potential antitumor activity, require their in vitro expansion. To avoid the potential dangers posed to patients by fetal bovine serum (FBS), the authors evaluated non-FBS culture conditions for the selective and efficient expansion of human Vα24+ NKT cells. Mononuclear cells (MNCs) and plasma from the peripheral blood of normal healthy donors were used before and after G-CSF mobilization. MNCs and plasma separated from apheresis products were also used. MNCs were cultured for 12 days in AIM-V medium containing α-galactosylceramide (α-GalCer) (100 ng/mL) and IL-2 (100 U/mL) supplemented with FBS, autologous plasma, or autologous serum. The cultured cells were collected and their surface markers, intracellular cytokines, and cytotoxicity were evaluated. The highest expansion ratio for Vα24+ NKT cells was obtained from G-CSF-mobilized MNCs cultured in medium containing 5% autologous plasma. Cultures containing MNCs and autologous plasma obtained before and after G-CSF mobilization had approximately 350-fold and 2,000-fold expansion ratios, respectively. These results suggest that G-CSF mobilization conferred a proliferative advantage to Vα24+ NKT cells by modifying the biology of cells and plasma factors. Expanded Vα24+ NKT cells retained their surface antigen expression and production of IFN-γ and exhibited CD1d-independent cytotoxicity against tumor cells. Vα24+ NKT cells can be efficiently expanded from G-CSF-mobilized peripheral blood MNCs in non-FBS culture conditions with α-GalCer and IL-2.

Key Words: NKT cells, G-CSF, α-galactosylceramide

(*J Immunother* 2005;28:314–321)

Received for publication August 13, 2004; accepted March 10, 2005.

From the *Hematopoietic Stem Cell Transplant/Immunotherapy Unit, National Cancer Center Hospital, Tokyo, Japan; †Pharmacology Division, Research Institute of National Cancer Center, Tokyo, Japan; ‡Kirin Brewery Company, Tokyo, Japan; §Department of Obstetrics and Gynecology, Toyama Medical and Pharmaceutical University, Toyama, Japan; and ‖National Cancer Center, Tokyo, Japan.

Supported by a Grant-in-Aid for Scientific Research from the Ministry of Health, Labor and Welfare in Japan.

Reprints: Yuji Heike, MD, PhD, Pharmacology Division, National Cancer Center Research Institute, Blood and Stem Cell Transplantation Unit, National Cancer Center Hospital, 1-1, Tsukiji 5-Chome, Chuo-Ku, Tokyo, 104-0045, Japan (e-mail: yheike@gan2.res.ncc.go.jp).

Murine Vα14+ natural killer (NK) T cells express an extremely restricted T-cell receptor (TCR) consisting of a Vα14-Jα281 α chain paired mainly with a Vβ8.2 β chain. Human Vα24+ NKT cells are similar to murine Vα14+ NKT cells, as Vα24+ NKT cells have an invariant Vα24-JαQ α chain preferentially paired with a Vβ11 chain.[1–3] α-Galactosylceramide (α-GalCer) is a specific ligand for human Vα24+ NKT cells and murine Vα14+ NKT cells.[4] Both types of NKT cells are activated by α-GalCer presented by CD1d. After stimulation with α-GalCer, Vα24+ NKT cells exhibit CD1d-dependent cytotoxicity against various types of tumor cells.[5–7] Because CD1d is probably a class I molecule expressed mainly on antigen-presenting cells (APCs) such as dendritic cells, macrophages, and B cells, it is speculated that NKT cells primarily interact with APCs.[6,8,9] NKT cells regulate innate tumor immunity by rapidly producing a large amount of IFN-γ and IL-4.[4,10]

The extremely low frequency of Vα24+ NKT cells in human peripheral blood[7,11,12] is an obstacle for their clinical application. To overcome this problem, the establishment of an effective in vitro expansion system for Vα24+ NKT cells by stimulation with α-GalCer has been explored. Significant expansion was reported in human Vα24+ Vβ11+ NKT cells cultured with a combination of IL-15, IL-7, IL-2, and α-GalCer.[13] Up to a 76-fold expansion of human Vα24+ Vβ11+ NKT cells was reported after culture with IL-7, IL-15, and α-GalCer-loaded monocyte-derived dendritic cells.[14] Alternative expansion methods use a combination of IL-2 and IL-15,[15] or α-GalCer and IL-2, with or without APCs.[16] Previously, we observed that Vα24+ NKT cells could be expanded 350-fold from human granulocyte-colony stimulating factor (G-CSF)–mobilized peripheral blood cells, upon stimulation with α-GalCer and IL-2 for 12 days.[17] However, in these culture systems, 10% fetal bovine serum (FBS) was used in the medium. To remove the potential risks related to FBS, we developed an efficient non-FBS expansion system for Vα24+ NKT cells.

MATERIALS AND METHODS

Cells, Plasma, and Serum Preparation

Peripheral blood and apheresis products were obtained from normal healthy individuals who were donating peripheral blood stem cells for allogeneic transplants. Written informed consent was obtained from the donors. This study was approved by our institution. Before and after G-CSF mobilization, samples were used immediately and cell fraction and

plasma were separated by centrifugation. The plasma and serum were obtained and cryopreserved at −80°C until use. Plasma and serum samples were heat-inactivated immediately before use. Mononuclear cells (MNCs) were isolated from peripheral blood and apheresis products by Ficoll-Hypaque (Immuno-Biologic Laboratories, Gunma, Japan) density gradient centrifugation. Apheresis plasma was also collected from the apheresis bags and used after heat inactivation.

G-CSF Procedure for Apheresis Donor

The apheresis was indicated for a healthy donor whose relative needed peripheral blood stem cell transplantation. This indication was checked by the clinical team of stem cell transplantation unit in our hospital. G-CSF was administered subcutaneously at a dosage of 300 μg/m^2 divided twice daily for 3 days just before the apheresis procedure. On the day of apheresis, one more dose of G-CSF was administered in the morning before apheresis.

Expansion of Vα24$^+$ NKT Cells

MNCs were cultured in six-well culture plates or culture flasks (Costar, Corning, NY) at 1.0×10^5 cells/mL in medium supplemented with 100 ng/mL α-GalCer (Kirin Brewery Co, Tokyo, Japan) and 100 U/mL recombinant human (rh) IL-2 (R&D Systems, Minneapolis, MN) for 12 to 14 days. The environment for the incubation was under 20% O_2 and 5% CO_2. Cells were cultured in AIM-V (Life Technologies, Rockville, MD) supplemented with 10% FBS (Hyclone, Logan, UT), 10% recombinant human serum albumin (rHSA), 5% or 10% autologous plasma, or 5% or 10% autologous serum. The rHSA was kindly provided by Mitsubishi Welpharma Corporation (Osaka, Japan). Fresh IL-2 was added every 3 days.

Co-Culture and Expansion of Vα24$^+$ NKT Cells

To determine whether G-CSF mobilization conferred any benefits to plasma or cells for the expansion of Vα24$^+$ NKT cells, we tested the following culture conditions: (1) pre-G-CSF peripheral blood mononuclear cells (PBMCs) cultured in AIM-V with 5% pre-G-CSF plasma; (2) pre-G-CSF PBMCs cultured in AIM-V with 5% post-G-CSF plasma; (3) post-G-CSF PBMCs cultured in AIM-V with 5% pre-G-CSF plasma; and (4) post-G-CSF PBMCs cultured in AIM-V with 5% post-G-CSF plasma. After culturing cells with α-GalCer and IL-2 for 12 days, we quantified the expansion of Vα24$^+$ NKT cells.

Cell Surface Antigen Analysis

We used mouse anti-human mAbs conjugated with fluorescein isothiocyanate (FITC), phycoerythrin (PE), allophycocyanin (APC), or peridinium chlorophyll (PerCP). CD3-PE, CD4-PerCP, CD8-PE, CD14-FITC, CD19-PE, CD25 (IL-2 receptor α chain)-FITC, and CD123 (IL-3 receptor)-PE mAbs were purchased from BD Biosciences (Mountain View, CA). Vα24-FITC, Vα24-PE, Vβ11-PE, CD124 (IL-4 receptor α chain)-PE, and CD127 (IL-7 receptor)-PE mAbs were purchased from Immunotech (Marseille, France). CD161-APC, CD114 (G-CSF receptor)-PE, and CD119 (IFN-γ recep-tor α chain)-PE mAbs were purchased from BD Pharmingen (San Diego, CA). PE-conjugated α-GalCer-CD1d tetramer was produced in our laboratory[18] and used to stain α-GalCer-loaded CD1d-reactive Vα24$^+$ NKT cells. Biotinylated anti-CD1d-mAb, which was originally produced by Dr. Steven A. Porcelli (Albert Einstein College of Medicine, Bronx, NY), was a kind gift from Kirin Brewery Co. The biotinylated mAb was detected using streptavidin-PerCP (BD Biosciences). For cell surface antigen staining, cells were incubated with mAbs for 30 minutes on ice. After staining, cells were washed twice and resuspended in PBS. Propidium iodide (Sigma-Aldrich, St. Louis, MO) staining preceded all experiments to remove dead cells. Data were acquired by flow cytometry (FACSCalibur; BD Biosciences) and analyzed using CellQuest software (BD Biosciences).

Vα24$^+$ NKT Cell Separation

After expansion of Vα24$^+$ NKT cells with α-GalCer and IL-2 in AIM-V with 5% autologous apheresis plasma for 12 days, cells were stained with Vα24-FITC for 20 minutes on ice and washed twice with 5 mM EDTA-PBS. After being incubated with anti-FITC microbeads (Miltenyi Biotec, Gladbach, Germany), Vα24$^+$ NKT cells were sorted by a magnetic cell separation system (Super MACS; Miltenyi Biotec), according to the manufacturer's protocol. After separation, the purity of isolated Vα24$^+$ NKT cells was determined to be more than 95% by flow cytometry. After the cells were re-cultured with 100 U/mL IL-2 for an additional 2 days, they were used for assays of cytotoxic activity against several tumor cell lines.

Intracellular Cytokine Assay

The intracellular cytokine production of cultured cells was measured by flow cytometry. Cells were activated with 10 ng/mL phorbol 12-myristate 13-acetate (Sigma-Aldrich) and 1 μg/mL ionomycin (Sigma-Aldrich) for 4 hours at 37°C in 10 μg/mL Brefeldin A (Sigma-Aldrich) to prevent cytokine secretion. After activation, cells were stained with Vα24 antigens and permeabilized according to the manufacturer's protocol (BD Biosciences) for staining with IFN-γ-PE or IL-4-PE mAb (BD Biosciences). At least 30,000 gating events per sample were acquired by FACSCalibur, and the data were analyzed using CellQuest software.

Cytotoxicity Assay

The cytotoxicity of isolated Vα24$^+$ NKT cells against tumor cell lines was studied. The following cell lines were purchased from ATCC: Daudi (B-cell lymphoma), K562 (chronic myelogenous leukemia), and Jurkat (T-cell lymphoma).

Target cells were labeled with 50 μCi sodium [^{51}Cr] chromate (NEN Life Science Products, Inc, Boston, MA) per 5×10^5 cells for 1 hour, washed three times, and resuspended at 1×10^5 cells/mL in medium. Next, 100 mL of effector cells and 100 mL of ^{51}Cr-labeled target cells (1×10^4 cells/well) were added to 96-well round-bottomed plates (Nunc, Roskilde, Denmark) at effector-to-target (E/T) ratios of 10:1, 3:1, and 1:1. Plates were incubated for 4 hours at 37°C, and ^{51}Cr release from lysed target cells was measured by a gamma counter. The percentage of specific ^{51}Cr released in each well was analyzed using the following formula: specific lysis (%) = (test cpm − spontaneous cpm)/(total cpm − spontaneous cpm) × 100. "Test cpm" indicates the counts in experimental cultures of target cells and effector cells; "spontaneous cpm" indicates the counts in cultures containing only target cells and medium;

and "total cpm" indicates the counts obtained by adding 100 mL of 1 N HCl to target cells to lyse all cells. Data are expressed as the mean and standard deviation of triplicate cultures.

ELISA

Levels of IL-2, IL-3, IL-4, IL-7, IL-13, IL-15, IFN-γ, and G-CSF in pre-G-CSF peripheral blood plasma and apheresis plasma were measured by commercial ELISA kits according to the manufacturers' protocols. IL-12 levels were measured by OptEIA (BD Pharmingen), and the other cytokine levels were measured by Immunoassay ELISA kits (BioSource, Camarillo, CA).

Statistical Analysis

The Student *t* test was used to compare groups using the two-tailed method dealing with dependent samples. $P < 0.05$ was considered statistically significant. In multiple group analysis, we adapted Bonferroni adjustment to confirm the significance of *P* values.

RESULTS

Efficient Expansion of Vα24$^+$ NKT Cells in Autologous Plasma

In this study, Vα24$^+$ CD3$^+$ cells were defined as Vα24$^+$ NKT cells. In our preliminary experiments using anti-Vβ11 mAb, we found that expanded Vα24$^+$ NKT cells fully express Vβ11. To search for a suitable non-FBS medium for Vα24$^+$ NKT cell expansion, PBMCs were cultured in medium containing α-GalCer, IL-2, and 10% FBS, 10% rHSA, 5% autologous plasma or serum, or 10% autologous plasma or serum for 12 to 14 days. The percentage of cultured Vα24$^+$ NKT cells increased by 27-fold in 10% FBS, 2-fold in 10% rHSA, 342-fold in 10% autologous plasma, 382-fold in 5% autologous plasma, 315-fold in 10% autologous serum, and 355-fold in 5% autologous serum (n = 5). Representative flow cytometry data are shown in Figure 1. When cells were cultured in medium containing 10% FBS, the percentage of expanded Vα24$^+$ NKT cells was substantially lower than when autologous plasma or autologous serum was used to supplement medium. In medium containing rHSA, the Vα24$^+$ NKT cells were unable to proliferate, whereas CD3$^+$ T cells proliferated. There was no significant difference between Vα24$^+$ cell expansion in 5% or 10% autologous plasma or autologous serum. Additionally, 87% to 95% of Vα24$^+$ NKT cells reacted to the α-GalCer-CD1d tetramer after expansion in 5% autologous plasma. These results suggest that medium containing 5% autologous plasma is suitable for selective expansion of Vα24$^+$ NKT cells with α-GalCer and IL-2 in vitro.

G-CSF Mobilization Augmented Vα24$^+$ NKT Cell Expansion

To develop more efficient plasma-based culture conditions for Vα24$^+$ NKT cells, we collected PBMCs and plasma before and after G-CSF mobilization (n = 18) and compared their expansion efficiencies (Table 1). Vα24$^+$ NKT cells significantly expanded to 1,938 (±2,501)-fold in the post-G-CSF condition compared with 346 (±345)-fold in the pre-G-CSF condition ($P = 0.018$). Thus, the Vα24$^+$ NKT cell expansion was 5.6-times greater in the post-G-CSF condition than in the pre-G-CSF condition. As the total cell number including all cell populations was not significantly different between the two cultures, the addition of α-GalCer in the post-G-CSF condition appeared to selectively expand Vα24$^+$ NKT cells.

Characteristics of G-CSF-Mobilized PBMCs and Plasma

To elucidate the contributions of G-CSF-mobilized PBMCs and plasma to Vα24$^+$ NKT cell expansion, different combinations of PBMCs and plasma from pre- and post-GCSF peripheral blood were tested (n = 8) (Fig. 2). Post-G-CSF plasma enhanced Vα24$^+$ NKT cell expansion more than pre-G-CSF plasma. Likewise, more Vα24$^+$ NKT cell proliferation occurred in post-G-CSF PBMCs than in pre-G-CSF PBMCs. The most effective combination was post-G-CSF PBMCs and post-G-CSF plasma. Exogenous G-CSF did not enhance the effective expansion of NKT cells (data not shown). These results suggest that G-CSF mobilization indirectly contributed to both PBMCs and plasma for the expansion of Vα24$^+$ NKT cells.

G-CSF Did Not Increase the Percentage of Vα24$^+$ NKT Cells in Peripheral Blood

We compared the percentages of Vα24$^+$ NKT cells in peripheral blood before and after G-CSF mobilization (n = 10). The percentage of Vα24$^+$ NKT cells in peripheral blood was 0.128% (±0.034) and was reduced to 0.082% (±0.040) by G-CSF mobilization ($P < 0.001$), although the absolute number of Vα24$^+$ NKT cells was similar in pre- and post-G-CSF peripheral blood—4.32 (±2.97) counts/μL and 6.03 (±3.41) counts/μL ($P > 0.05$), respectively. This means that mobilized PBMCs contain a high proportion of monocyte, which resulted in decreasing the percentage of Vα24$^+$ NKT cells relatively. As the total number of Vα24$^+$ NKT cells in peripheral blood did not change, therefore the Vα24$^+$ NKT cells were not mobilized by G-CSF administration.

G-CSF-Induced Changes in Peripheral Blood Cytokine Concentrations

We measured cytokine concentrations in the plasma of pre-G-CSF and apheresis products (n = 6) (Fig. 3). The level of G-CSF increased dramatically after G-CSF administration. There were significant differences between the levels of three cytokines (IL-3, IL-7 and IL-13) between apheresis products and pre-G-CSF plasma. The levels of other cytokines, such as IL-2, IL-12, IL-15, and IFN-γ, which enhance Vα24$^+$ NKT cell function, were not changed by G-CSF mobilization. The concentrations of IL-4 were below the detection limit.

Expression of Cytokine Receptors on T Cells and NKT Cells After G-CSF Mobilization

We evaluated the expression of cytokine receptors for IL-2, IL-3, IL-4, IL-7, G-CSF, and IFN-γ on CD3$^+$ T cells and Vα24$^+$ NKT cells in pre- and post-G-CSF PBMCs (n = 5) (Fig. 4). The expression levels of IL-3, IL-7, and IL-4 receptor (which has IL-13 common receptor[19]) on CD3$^+$ T cells and Vα24$^+$ NKT cells were not affected by G-CSF mobilization, although the corresponding cytokine levels (IL-3, IL-7, and

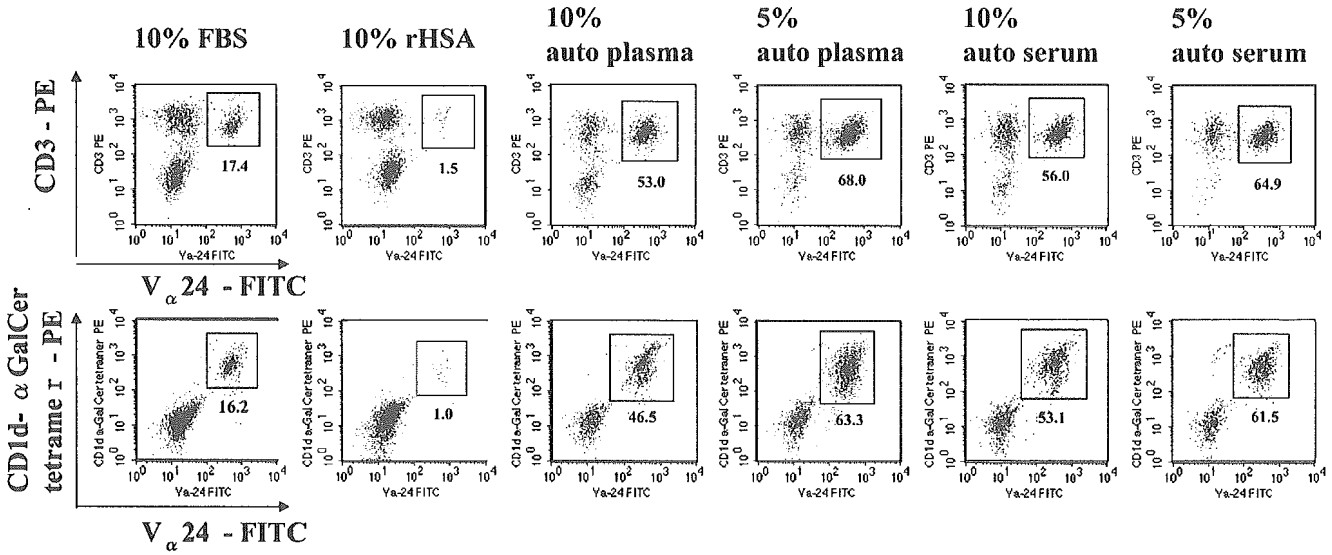

FIGURE 1. Differences in Vα24+ NKT cell expansion according to the type of supplemented protein. PBMCs from normal healthy donors were cultured for 12 to 14 days with α-GalCer and IL-2 in the presence of 10% FBS, 10% rHSA, 5% or 10% autologous plasma, or 5% or 10% autologous serum. Vα24+ CD3+ cells were defined as Vα24+ NKT cells. Vα24+ CD1d-α-GalCer tetramer-positive NKT cells were also stained, and the percentage of the gated population is shown. These flow cytometry results are representative of five independent experiments.

IL-13) were increased by G-CSF mobilization. The IL-7 receptor was expressed on most Vα24+ NKT cells, although some CD3+ T cells showed downregulation of the IL-7 receptor after G-CSF mobilization. There was no obvious tendency for G-CSF mobilization to enhance the expression level of the G-CSF receptor or the α chain of the IL-2 receptor on both CD3+ T cells and Vα24+ NKT cells. Interestingly, only the α chain of the IFN-γ receptor increased after G-CSF mobilization with a significant difference ($P = 0.009$), and this increase occurred on Vα24+ NKT cells but not on CD3+ T cells.

Cell Populations

Table 2 shows mean values and standard deviations for the cell kinetics of apheresis MNCs cultured with autologous apheresis plasma (n = 11). The apheresis procedure did not affect the percentage of Vα24+ NKT cells. On day 0, Vα24+ NKT cells represented only 0.10% (± 0.06) of apheresis MNCs, and the CD4+ to CD8+ T-cell ratio was more than 1.0. Monocytes accounted for approximately 30% of MNCs at day 0, which was substantially higher than the percentage of monocytes (2.7–7.9%) in pre-G-CSF PBMCs. When stimulated with α-GalCer, Vα24+ NKT cells propagated linearly until day 14. CD8+ T cells expanded to become the predominant T-cell population, changing the CD4+ to CD8+ T-cell ratio to less than 1.0. B cells and monocytes almost completely disappeared by day 14 (2.33% and 0.16%, respectively).

TABLE 1. Comparison of Expansion Efficiencies

	Vα24+ NKT Cells			Whole Cells
	Day 0 (%)	Day 12–14 (%)	Expansion Fold	Day 12–14 (expansion fold)
Pre-G-CSF	0.19	10.45 ± 8.53	×345.96 ± 345	×5.33
Post-G-CSF	0.11	21.97 ± 11.70*	×1,938.11 ± 2,501*	×4.62

*$P < 0.05$.

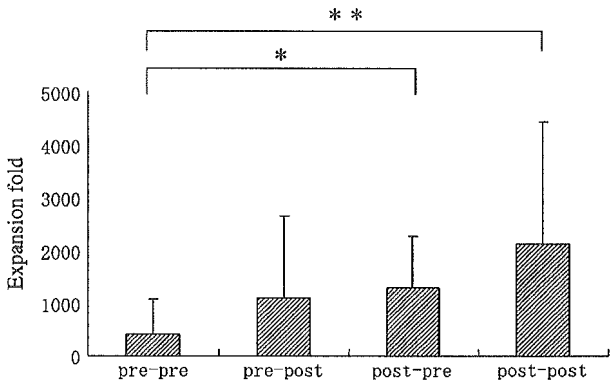

* P<0.05 both in t-test and Bonferoni adjustment,
** P<0.05 in t-test but not Bonferoni adjustment

FIGURE 2. Differences in Vα24+ NKT cell expansion influenced by a combination of PBMCs and plasma. The expansion of Vα24+ NKT cells was analyzed in several co-culture combinations of PBMCs and 5% plasma before and after G-CSF mobilization. Cells were cultured for 14 days in the presence of α-GalCer and IL-2. Values are the mean and standard deviation of the Vα24+ NKT cell expansion fold. Samples were obtained from the same donor (n = 8), and the following co-culture conditions were examined: (1) pre-G-CSF PBMCs and pre-G-CSF plasma (pre-pre); (2) pre-G-CSF PBMCs and post-G-CSF plasma (pre-post); (3) post-G-CSF PBMCs and pre-G-CSF plasma (post-pre); and (4) post-G-CSF PBMCs and post-G-CSF plasma (post-post). *$P < 0.05$. P values were determined using the Student t test and Bonferroni adjustment.

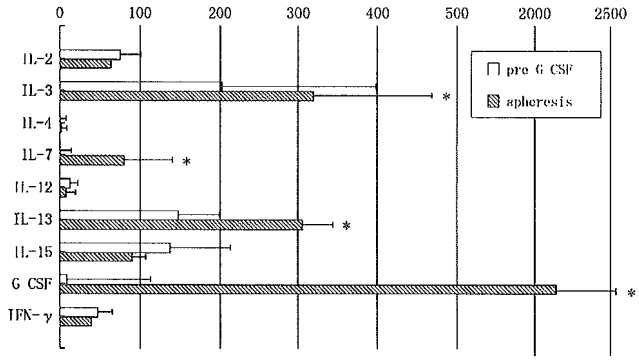

FIGURE 3. Cytokine levels in plasma. Cytokine levels in peripheral blood were measured by ELISA before G-CSF mobilization and in apheresis products from the same normal healthy donors (n = 6). IL-2 levels are plotted in U/mL; all other cytokine levels are plotted in pg/mL. Results are shown as mean values with standard deviations. *$P < 0.05$ vs. pre-G-CSF peripheral blood and apheresis product.

NK cells were also remarkably reduced after day 7, although they grew rapidly in the first 7 days of culture.

Cytokine Production

We measured IFN-γ and IL-4 production in apheresis MNCs (n = 10) that were cultured with or without α-GalCer for 14 days. Representative flow cytometry data are shown in Figure 5. The percentage of IFN-γ-producing MNCs was 58.7 ± 13.9% when cultured with α-GalCer and 44.8 ± 15.6% when cultured without α-GalCer. The percentage of IL-4-producing MNCs was 8.6 ± 8.5% when cultured with α-GalCer and 5.0 ± 2.9% when cultured without α-GalCer. When cultured with α-GalCer, 75.7 ± 12.2% of Vα24$^+$ NKT cells produced IFN-γ and 16.2 ± 10.5% produced IL-4. In the comparison of IFN-γ and IL-4 produced by Vα24$^+$ NKT cells, IFN-γ was significantly dominant ($P = 0.023$).

Cytotoxicity Assays

Three tumor cell lines were used as target cells in the cytotoxic assay. CD1d expression on the target tumor cells was evaluated using CD1d mAb. CD1d was expressed on 87% of Jurkat cells and 13% of Daudi cells. K-562 did not express CD1d. Vα24$^+$ NKT cells purified from MNCs stimulated with α-GalCer mediated strong cytotoxic effects against all of these hematologic cell lines (Fig. 6). The cytotoxicities were unrelated to CD1d expression on the target cells.

DISCUSSION

NKT cells help regulate a variety of immune responses, including the immune responses associated with autoimmune diseases,[20] including inflammatory bowel disease,[21] graft-versus-host disease,[22] and tumor rejection.[23] Two main strategies have been devised to use the specific ligand for NKT cells, α-GalCer, in therapeutic settings: the in vivo use of α-GalCer to enhance an immune response and the ex vivo use of α-GalCer to expand NKT cells for adoptive transfer. When the former approach was tested in patients with various solid tumors,[24] there were short-term elevations in IL-12 and GM-CSF levels and NK cell activity, and a slight elevation in serum IFN-γ and IL-4 levels occurred in some patients. Interestingly, the NKT cells disappeared from peripheral blood within 24 hours of α-GalCer injection. Although no adverse events were associated with this approach, no therapeutic benefits were apparent either. In murine models, high doses of α-GalCer showed significant liver toxicity.[25]

Nieda et al[16] studied the alternative approach of the infusion of α-GalCer-pulsed dendritic cells. They reported a transient decrease in the number of Vα24$^+$ Vβ11$^+$ NKT cells in the peripheral blood within 48 hours of the infusion. This transient decrease was followed by significant increases in Vα24$^+$ Vβ11$^+$ NKT cells and the serum levels of IFN-γ and IL-12, in addition to the activation of NK cells and T cells. No significant adverse events were reported in a clinical trial of this approach.[26]

The clinical use of Vα24$^+$ NKT cells requires the development of a highly effective expansion method for Vα24$^+$ NKT cells ex vivo. Previous reports of ex vivo cell expansion for clinical applications have focused on T cells,[27,28] NK cells,[29] or dendritic cells[30] rather than NKT cells. A few reports have found that the expansion of human NKT cells from steady-state peripheral blood cells or cord blood cells can be mediated by α-GalCer and several cytokines.[13–16] However, the expansion ratios of these NKT cells were limited. Our previous study showed that G-CSF-mobilized peripheral blood cells, whether from normal donors or cancer patients, had a significantly higher expansion potential for Vα24$^+$ NKT cells in a combination culture of α-GalCer and IL-2.[17] These results provide a realistic rationale for performing adoptive transfer of α-GalCer-expanded Vα24$^+$ NKT cells in combination with high-dose chemotherapy and G-CSF treatment or in combination with autologous or allogeneic hematopoietic stem cell transplantation including G-CSF mobilization. Nevertheless, these approaches are seriously limited by the use of FBS, and the development of a non-FBS culture system is critical.

In the present study, we tested a culture system that uses autologous plasma for the expansion of Vα24$^+$ NKT cells in the presence of α-GalCer and IL-2. We also evaluated the sustained usefulness of G-CSF-mobilized specimens. We found that autologous serum and autologous plasma had greater capacities to expand Vα24$^+$ NKT cells than did FBS and rHSA. Indeed, there was no significant difference between Vα24$^+$ NKT cell expansion in 5% or 10% autologous plasma or autologous serum. However, the percentage of Vα24$^+$ cells in culture medium was the highest and 87% to 95% of Vα24$^+$ NKT cells reacted to the α-GalCer-CD1d tetramer after expansion in 5% autologous plasma. Additionally, plasma can easily be obtained in the process of PBMC preparation from peripheral blood samples and in the process of apheresis. Thus, we selected plasma as a medium supplement. We also found that G-CSF-mobilized PBMCs and G-CSF-mobilized plasma, which were used instead of steady-state PBMCs and plasma, yielded the highest expansion ratio for Vα24$^+$ NKT cells. When we comparatively analyzed cells and plasma before and after G-CSF mobilization, we found that both G-CSF-mobilized PBMCs and G-CSF-mobilized plasma had the capability to support expansion of Vα24$^+$ NKT cells (see

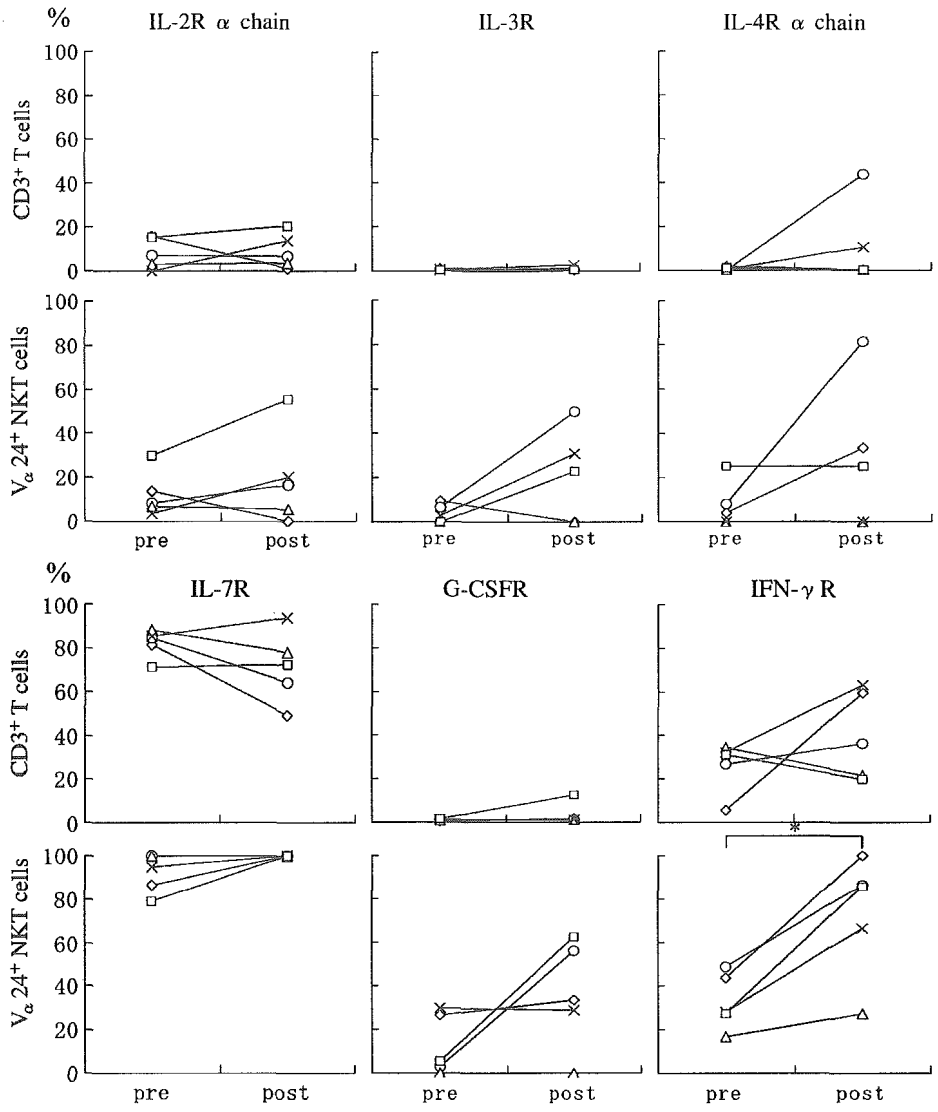

FIGURE 4. Cytokine receptor expression. Changes in the cytokine receptor expression of $CD3^+$ T cells and $V\alpha24^+$ NKT cells in peripheral blood before and after G-CSF mobilization are shown as five independent experiments. Peripheral blood before and after G-CSF-mobilization was obtained from the same healthy donors. Figure symbols indicate individual donors. $^*P < 0.05$.

Fig. 2). In the clinical setting, we plan to use mobilized PBMCs and apheresis product derived from cancer patients in the autologous setting or derived from a healthy donor in the allogeneic setting. The clinical application of ex vivo expanded NKT cells has a possibility of wide modification, including combination therapy with stem cell transplantation.

TABLE 2. Cell Kinetics of Apheresis MNCs Cultural with Autologous Apheresis Plasma

Cell Population	Day 0	Day 7	Day 14
$V\alpha24^+$ $CD3^+$ (NKT)	0.10 ± 0.06	12.90 ± 15.15	21.77 ± 21.68
$CD3^-$ $CD161^+$ (NK)	3.41 ± 2.08	26.03 ± 15.47	8.79 ± 6.85
$CD161^-$ $V\alpha24^-$ $CD4^+$ (CD4 T)	18.57 ± 7.53	18.07 ± 7.02	16.91 ± 12.28
$CD161^-$ $V\alpha24^-$ $CD8^+$ (CD8 T)	12.42 ± 3.42	26.71 ± 12.28	23.69 ± 12.20
$CD19^+$ (B cell)	7.40 ± 4.30	5.62 ± 3.27	2.33 ± 2.06
$CD14^+$ (monocyte)	29.39 ± 15.58	0.93 ± 1.12	0.16 ± 0.16

Data are given as percentages ± SD.

Contrary to our expectations, our flow cytometry data revealed that the percentage of $V\alpha24^+$ NKT cells in vivo decreased after G-CSF mobilization. As the absolute number of $V\alpha24^+$ NKT cells did not change by G-CSF mobilization, the decreased percentage of it was caused by the increment of other cell populations after G-CSF mobilization. That means that G-CSF does not mobilize $V\alpha24^+$ NKT cells directly. Also, ex vivo supplementation of G-CSF did not enhance the expansion of $V\alpha24^+$ NKT cells (data not shown), which suggests an indirect contribution of G-CSF in the expansion of NKT cells, contrary to a previous report.[31] On the other hand, the post-G-CSF PBMCs (see Table 2) and apheresis products contained a high percentage of monocytes, which include APCs capable of presenting α-GalCer. This observation indicates that the number of CD1d-expressing PBMCs also increased after G-CSF mobilization and might be one factor responsible for the significant expansion of $V\alpha24^+$ NKT cells in post-G-CSF

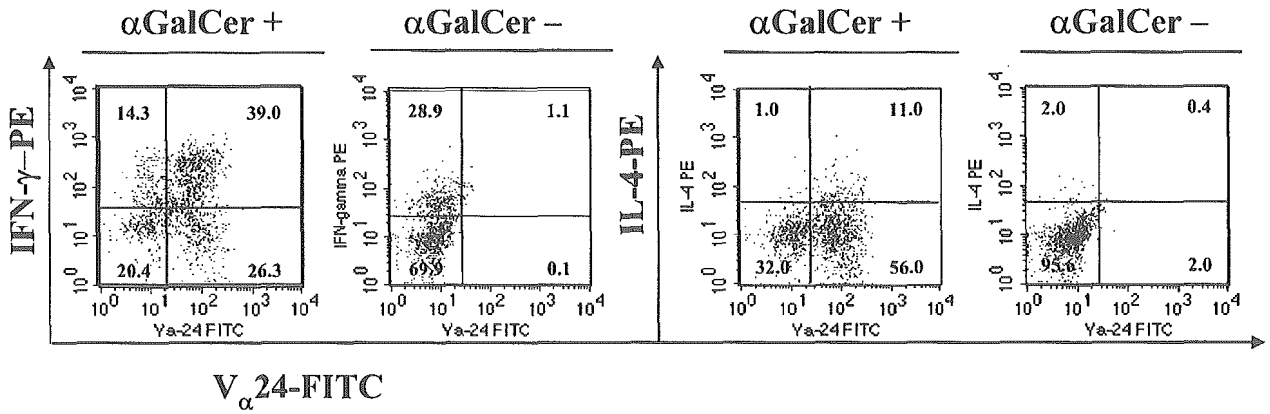

FIGURE 5. Intracellular cytokines in cultured Vα24$^+$ NKT cells. Intracellular IFN-γ and IL-4 were stained in whole cells after culture with or without α-GalCer. Cells were activated with phorbol 12-myristate 13-acetate and ionomycin for 4 hours. Representative data from 1 of 10 independent experiments are presented. *$P < 0.05$, difference between the production of IFN-γ and IL-4, Student t test.

PBMCs. We previously reported that cell-to-cell contact with CD14$^+$ cells was needed for the expansion of NKT cells.[17]

The plasma collected after G-CSF mobilization also had an enhanced capacity for Vα24$^+$ NKT cell expansion. IL-2, IL-7, IL-12, IL-15, IL-18, and IFN-γ directly induce proliferation and activation of NKT cells.[13,14,32,33] However, none of these cytokines, with the exception of IL-7, was increased in the plasma of G-CSF-mobilized peripheral blood. When Vα24$^+$ NKT cells were cultured with α-GalCer and increased levels of cytokines (IL-3, IL-7, IL-13, and G-CSF) in medium containing pre-G-CSF plasma, the expansion efficiency of Vα24$^+$ NKT cells was not enhanced to the level achieved with post-G-CSF plasma (data not shown). These results suggest that IL-3, IL-7, IL-13, and G-CSF do not directly contribute to the proliferation of Vα24$^+$ NKT cells. The identification of these unknown factors in post-G-CSF plasma, which promote the proliferation of Vα24$^+$ NKT cells, would increase the effectiveness of Vα24$^+$ NKT cell expansion.

To determine whether the characteristics of cells were changed by G-CSF mobilization, we evaluated the expression of several cytokine receptors on CD3$^+$ T cells and Vα24$^+$ NKT cells isolated from peripheral blood before and after G-CSF mobilization. A significant increase was observed in the expression of the IFN-γ receptor α chain on Vα24$^+$ NKT cells after G-CSF mobilization ($P = 0.009$). This increased α-chain expression may be partially responsible for the proliferative advantage of Vα24$^+$ NKT cells after G-CSF mobilization. However, the variability of response between individuals is essential issue, especially in the evaluation of receptor intensity. This variation suggests that the ex vivo expansion of NKT cells is controlled by mutual change, which exists in cellular and humoral factor.

We found that expanded Vα24$^+$ NKT cells predominantly produced IFN-γ. The expanded Vα24$^+$ NKT cells exhibited augmented cytotoxicity against CD1d$^+$ tumor cell lines (Daudi and Jurkat) as well as CD1d$^-$ tumor cell line (K562). In CD1d-blocking experiments, we found that expanded Vα24$^+$ NKT cells mediated cytotoxic activity against CD1d-blocked Jurkat cells that was comparable to the cytotoxic activity against CD1d-unblocked Jurkat cells (data not shown). Thus, the expanded Vα24$^+$ NKT cells yielded lytic activity against tumor cells in a CD1d-independent manner. Although the mechanism of CD1d-related cytotoxicity mediated by Vα24$^+$ NKT cells has not been clarified, other recent studies of NKT cells suggest that CD1d expression on the target tumor cells is not essential for cytotoxicity.[34–36] The Vα24$^+$ NKT cells

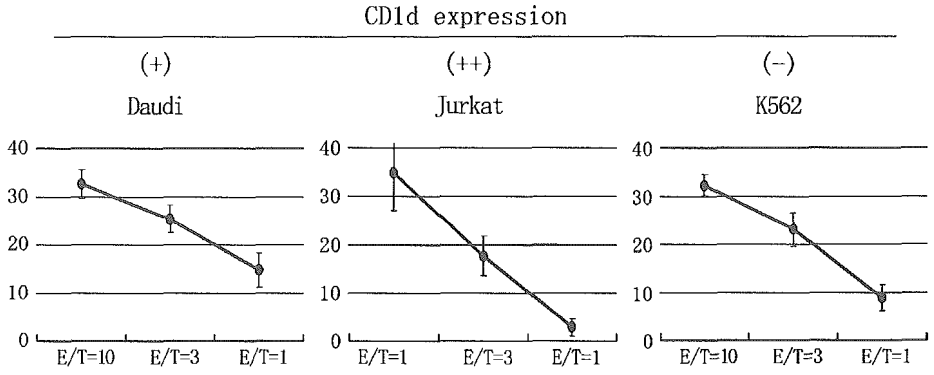

FIGURE 6. Cytotoxicity of purified Vα24$^+$ NKT cells after culture. Vα24$^+$ NKT cell-mediated cytotoxicity against tumor cells was measured with effector-to-target ratios of 10:1, 3:1, and 1:1. Cell lines were classified into the following four groups based on the expression level of CD1d: (-), 0–3%; (±), 3–10%; (+), 10–60%; (++), 60–100%. Cytotoxicity was evaluated with ^{51}Cr release assays. The means and standard deviations of triplicate culture are shown in representative result of four independent experiments.